Title
14-3-3 adaptor proteins recruit AID to 5′-AGCT-3′–rich switch regions for class switch recombination

Journal
Nature Structural & Molecular Biology, 17(9)

ISSN
1545-9993

Authors
Xu, Zhenming
Fulop, Zsolt
Wu, Guikai
et al.

Publication Date
2010-09-01

DOI
10.1038/nsmb.1884

HHS Public Access

Author manuscript

Nat Struct Mol Biol. Author manuscript; available in PMC 2013 May 06.

Published in final edited form as:

Nat Struct Mol Biol. 2010 September ; 17(9): 1124–1135. doi:10.1038/nsmb.1884.

14-3-3 adaptor proteins recruit AID to 5′-AGCT-3′-rich switch regions for class switch recombination

Zhenming Xu[1], **Zsolt Fulop**[1,§], **Guikai Wu**[2], **Egest J. Pone**[1], **Jinsong Zhang**[1], **Thach Mai**[1], **Lisa M. Thomas**[1], **Ahmed Al-Qahtani**[1], **Clayton A. White**[1], **Seok-Rae Park**[1,¶], **Petra Steinacker**[3], **Zenggang Li**[4], **John Yates III**[5], **Bruce Herron**[6], **Markus Otto**[3], **Hong Zan**[1], **Haian Fu**[4], and **Paolo Casali**[1]

[1]Institute for immunology, School of Medicine and School of Biological Sciences, University of California, Irvine, CA 92697-4120

[2]Department of Biological Chemistry, School of Medicine, University of California, Irvine, CA 92697

[3]Department of Neurology, University of Ulm, 89075 Ulm, Germany

[4]Department of Pharmacology, School of Medicine, Emory University, Atlanta, GA 30322

[5]Department of Chemical Physiology, The Scripps Research Institute, La Jolla, CA 92037

[6]Wadsworth Center, New York State Department of Health, Albany, NY 12201

Abstract

Class switch DNA recombination (CSR) is the mechanism that diversifies the biological effector functions of antibodies. Activation-induced cytidine deaminase (AID), a key CSR player, targets IgH switch (S) regions, which contain 5′-AGCT-3′ repeats in their core. How AID is recruited to S regions remains unclear. Here we show that 14-3-3 adaptor proteins play an important role in CSR. 14-3-3 proteins specifically bind 5′-AGCT-3′ repeats, are upregulated in B cells undergoing CSR and are recruited together with AID to the S regions involved in CSR events (Sμ→Sγ1, Sμ→Sγ3 or Sμ→Sα). Moreover, blocking 14-3-3 by difopein, deficiency in 14-3-3γ or expression of a dominant negative 14-3-3σ mutant impaired recruitment of AID to S regions and decreased CSR. Finally, 14-3-3 proteins interact directly with AID and enhance AID-mediated *in vitro* DNA deamination, further emphasizing the important role of these adaptors in CSR.

Correspondence should be addressed to Paolo Casali (pcasali@uci.edu; phone: 949-824-9648; fax: 949-824-2305).

§Present address: Department of Gastroenterology, St John's Hospital and United Hospitals of Northern Buda of the Metropolitan Government, H-1032, Budapest, Hungary.

¶Present address: Department of Microbiology, College of Medicine, Konyang University, Daejeon 302-801, Republic of Korea.

Author Contributions: Z.X., Z.F., G.W., E.J.P., J.Z., T.M., L.M.T., A.A.-Q., C.A.W., S.-R.P, Z.L. and H.Z. performed experimental work; J.R.Y. III was responsible for the MudPIT analysis; B.H. provided *14-3-3*$\sigma^{+/Er}$ mice; P.S. and M.O. provided *14-3-3*$\gamma^{-/-}$ mice; H.F. provided recombinant 14-3-3 proteins, 14-3-3 isoform-specific Abs and the difopein-expressing construct; H.Z. designed experiments; Z.X. designed experiments and prepared the manuscript; and P.C. designed experiments, supervised the project and prepared the manuscript.

Competing Interests Statements: The authors declare no competing financial interests.

Keywords

14-3-3; 14-3-3γ knockout (KO); 14-3-3σ mutant; activation-induced cytidine deaminase (AID); AGCT; B cell; BiFC; class switch DNA recombination (CSR); difopein; germinal center; immunoglobulin (Ig); multiple dimensional protein identification technology (MudPIT); repeated epilation; Sfn; switch (S) regions

Immunoglobulin (Ig) somatic hypermutation (SHM) and CSR are central to the maturation of the antibody response and occur mainly in B lymphocytes of germinal centers in secondary lymphoid organs[1]. SHM inserts mostly point-mutations in V(D)J region DNA at a high rate, thereby providing a structural basis for the generation of high affinity Ig mutants and their selection by antigen[2]. The SHM machinery preferentially targets the 5′-RGYW-3′ (R = A or G, Y = C or T and W = A or T) motif[3-6]. CSR substitutes an Ig heavy chain (IgH) constant (C_H) region, for instance, Cμ, with a downstream C_H region, Cγ, Cα or Cε, thereby endowing an antibody with different biological effector functions without changing the structure/specificity of the antigen-binding site. CSR is induced by engagement of B cell surface CD40 by T cell surface CD154 and exposure to cytokines, such as IL-4, IFN-γ or TGF-β. It can also be induced by T-independent stimuli, e.g., ligands of Toll-like receptors (TLRs)[7-9].

CSR entails IgH locus transcription, which is promoted by the I_H promoter (Iμ, Iγ, Iα or Iε) and goes through the S and C_H DNA of the recombining C_H regions to give rise to germline I_H-C_H (Iμ-Cμ, Iγ-Cγ, Iα-Cα or Iε-Cε) transcripts[7]. S regions are located 5′ of each of the C_H region genes, except for Cδ, and contain tandem motif repeats in their “core” sequences. CSR then proceeds through generation of double-strand DNA breaks (DSBs) in S regions, followed by deletion of the DNA intervening between the upstream and downstream S regions and re-ligation of DSB free-ends to form S-S junctions. Post-recombination DNA transcription gives rise to Iμ-Cγ, Iμ-Cα or Iμ-Cε transcripts[7]. The deleted intervening DNA is looped out to form extrachromosomal S DNA circles, which are transiently transcribed, giving rise to circle Iγ-Cμ, Iα-Cμ or Iε-Cμ transcripts, which are hallmarks of ongoing CSR to IgG, IgA or IgE[7].

Whether induced in T-dependent or T-independent fashion, CSR requires AID[10, 11], which is encoded by the *AICDA/Aicda* gene and is induced in a HoxC4-dependent fashion in B cells by the stimuli that induce CSR and SHM[12]. AID belongs to the AID/APOBEC cytosine deaminase family, whose other members, such as APOBEC3G and APOBEC3B, are associated with pathways of retroviral restriction[13]. Like APOBEC3G[14, 15], AID deaminates deoxycytidine (dC) in DNA[6, 16, 17]. After phosphorylation by PKA at Ser38, AID displays enhanced deamination of transcribed double-strand DNA in the presence of replication protein A (RPA)[18]. This together with findings on AID expression[5, 12, 19-21], stability[22, 23], subcellular localization[23-26] and enzymatic activities[6, 16, 27] have provided a good understanding of AID regulation. Nevertheless, how AID and the whole CSR machinery target S regions remains to be determined.

DSBs in S regions[28, 29] are effected by AID-mediated cytidine deamination, which gives rise to uracil (dU), dU deglycosylation by Ung[30] and further intervention of elements of the

BER pathway[7]. Resolution of S region DSBs is mediated by elements of the classical NHEJ and/or alternative NHEJ pathways, including the Mre11-Rad50-NBS1 complex[31-33]. Like SHM, DSBs and S-S junctions in CSR preferentially segregate within the 5′-RGYW-3′ motif, particularly its 5′-AGCT-3′ iteration[2, 29, 34-36]. 5′-AGCT-3′-rich *Xenopus laevis* (*X. laevis*) Sμ DNA effectively promoted CSR to IgG1 when grafted into the mouse to replace Sγ1[37] and, conversely, CSR was significantly impaired following deletion of the 5′-AGCT-3′-rich Sμ core[38]. Mouse Sγ1 and Sγ3 core DNA, as well as their respective inversions, all contain high numbers of 5′-AGCT-3′ repeats and could replace the full-length Sγ1 to mediate CSR to IgG1[39], further suggesting a role of 5′-AGCT-3′ repeats in targeting the CSR machinery, including AID, to S region DNA.

Here, we outline an important role of 14-3-3 adaptors in CSR. We have used affinity chromatography and multiple dimensional protein identification technology (MudPIT) to identify 14-3-3 adaptors as specifically binding to 5′-AGCT-3′ repeats. The seven mammalian 14-3-3 isoforms (14-3-3β, 14-3-3ε, 14-3-3γ, 14-3-3η, 14-3-3σ, 14-3-3τ and 14-3-3ζ), encoded by seven genes, are differentially expressed in a variety of cells[40]. They exhibit isoform-specific, but overlapping and redundant functions in regulating many cellular processes, including proliferation and (anti-apoptotic) survival[41]. Accordingly, cells with selective and/or partial deficiency in 14-3-3 isoforms displayed normal cell functions and proliferation[42]. Overcoming the redundancy of 14-3-3 isoforms in promoting these functions requires exposure of cells to harsh conditions, such as DNA damaging agents (for instance, ionizing irradiation[43]). Here, we have used B cells expressing the highly specific 14-3-3 inhibitor (difopein) and mice deficient/mutant in 14-3-3 isoforms to address the role of 14-3-3 in recruiting and/or stabilizing AID to S regions in CSR. We have also used bimolecular fluorescence complementation (BiFC) and *in vitro* DNA deamination assays involving recombinant AID and purified 14-3-3 isoforms to show that 14-3-3 proteins directly interact with AID and enhance AID-mediated DNA deamination.

Results

14-3-3 adaptors bind to 5′-AGCT-3′ repeats

5′-AGCT-3′ repeats recur at a high frequency in all human and mouse S regions, accounting for more than 45% of Sμ core DNA, but less than 1.4% of DNA in the genome at large, including C_H regions (Supplementary Table 1). 5′-AGCT-3′ repeats also recur at a high frequency in S regions of other species in which CSR occurs, including frog, rat, cow and horse (Supplementary Fig. 1; data not shown). This prompted us to use 5′-AGCT-3′ repeats as “bait” to identify proteins that specifically bind to S region DNA. We used a 24-bp DNA oligonucleotide, “$[5′\text{-AGCT-}3′]_3$–24 bp”, which contains three 5′-AGCT-3′ motifs separated by 5′-TTTT-3′, as the probe for EMSAs with nuclear extracts from human IgM^+ IgD^+ 4B6 B cells, which undergo spontaneous CSR to IgG, IgA and IgE[44]. We observed the formation of two protein/DNA complexes, A and A′, migrating as two discrete but close bands (Fig. 1a). Formation of these complexes was not observed with a control oligonucleotide containing repeats of 3′-AGCT-5′, the reverse isomer of 5′-AGCT-3′ (Fig. 1a). In addition, this control could not outcompete the $[5′\text{-AGCT-}3′]_3$–24 bp probe, even in 160-fold molar excess (Supplementary Fig. 2a). Further, the formation of A and A′ complexes could not be

disrupted by low pH (4.8) or high salt concentration (300 mM KCl) (Supplementary Fig. 2b). The specificity of these complexes is further demonstrated by the lack of binding to oligonucleotides containing the other seven iterations of 5′-RGYW-3′ (with only marginal binding to [5′-AGCA-3′]$_3$–24 bp) or 5′-GGGG-3′, the major constituent of 5′-GGGGT-3′, a motif frequently occurring in S regions[7] (Fig. 1b).

To isolate [5′-AGCT-3′]$_3$–24 bp-binding proteins, we applied 4B6 cell nuclear extract proteins to an affinity column bearing immobilized [5′-AGCT-3′]$_3$–24 bp oligonucleotide, in the presence of 100-fold molar excess of the control [3′-AGCT-5′]$_3$–24 bp oligonucleotide. After extensive washing, we eluted the proteins bound to the column with 600 mM NaCl and analyzed them by silver staining (Supplementary Fig. 2c). The elution fractions showed prominent protein bands at 28 kD and were subjected to high-throughput MudPIT analysis. This identified the seven 14-3-3 isoforms (β, ε, γ, η, σ, τ and ζ, 27.8 kD to 29.2 kD in size), which collectively accounted for more than half (52.8%, 59.2% and 50.7% in three independent experiments) of the total of eluted proteins (Fig. 1c) – the identity of the eluted 14-3-3 proteins was verified by immunoblotting (Supplementary Fig. 2d). By contrast, the twenty most abundant non-14-3-3 proteins collectively accounted for only 23.1% of the total proteins (Supplementary Table 2).

As all 14-3-3 isoforms form homo-/heterodimers, the protein/DNA complexes A and A′ likely reflected binding of the 5′-AGCT-3′ probe by 14-3-3 dimers of different compositions. Accordingly, pre-incubation of nuclear extracts from 4B6 B cells with different Abs recognizing all 14-3-3 isoforms either abrogated the formation of the complexes (Abs1 and 2) or supershifted such complexes (Abs 3 and 4); likewise, an Ab specific for 14-3-3ζ inhibited the formation of A and A′, and an Ab specific for 14-3-3β supershifted the complex A′ (Fig. 1d). Further, DNase I footprint showed that purified recombinant 14-3-3γ, 14-3-3σ and 14-3-3ζ selectively protected from DNase I digestion the three 5′-AGCT-3′ motifs but other sequences in a 126-bp oligonucleotide, thereby providing an internally-controlled confirmation of the specificity of 14-3-3 binding to 5′-AGCT-3′ (Fig 1e). Moreover, purified recombinant 14-3-3ζ directly bound to [5′-AGCT-3′]$_3$–24 bp in a dose-dependent fashion, and its binding was significantly reduced by an Ab to 14-3-3ζ or an Ab to all 14-3-3 isoforms. Finally, the K49E mutation of the 14-3-3ζ amphipathic groove, previously shown to bind to Raf-1[45] and suggested to bind dsDNA[46], reduced binding to [5′-AGCT-3′]$_3$–24 bp (Supplementary Fig. 2e,f).

Altogether, these results show that 14-3-3 adaptors are nuclear proteins that specifically bind to the 5′-AGCT-3′ repeats characteristic of human and mouse S regions.

14-3-3 proteins bind to the S regions involved in ongoing CSR

We decided to analyze the binding of 14-3-3 to S regions (rich in 5′-AGCT-3′) and to Cμ, which lies in the same (IgH) locus but contains far fewer 5′-AGCT-3′ motifs. We performed chromatin immunoprecipitation (ChIP) assays with human 4B6 B cell extracts and an Ab to 14-3-3, and detected Sμ, Sγ1 and Sα DNA, but not Cμ (or *PAX5*, as another control); we also detected Sμ, Sγ1 and Sα DNA in chromatin precipitated by Ab to AID (Fig. 2a). Likewise, we specified Sμ and Sγ1 DNA in chromatin precipitated by Ab to 14-3-3, AID or

RPA from IgM$^+$ IgD$^+$ 2E2 B cells after induction of CSR to IgG1 by mAb to human CD40 (hCD40) plus human IL-4 (hIL-4)[29] (Fig. 2a).

We next analyzed the binding of 14-3-3 and AID to S regions in mouse B cells undergoing CSR. Stimulation of IgM$^+$ CH12F3 B cells by LPS plus mouse IL-4 (mIL-4) and TGF-β induced CSR to IgA, but not IgG1[47], and binding of 14-3-3 and AID to Sμ and Sα DNA, but not Sγ1 DNA (Fig. 2b). In mouse primary B cells, LPS-induced CSR to IgG3 was associated with the binding of 14-3-3 and AID to Sμ and Sγ3 DNA, but not Sγ1 DNA. Conversely, LPS plus mIL-4-induced CSR to IgG1 was associated with the binding of 14-3-3 and AID to Sμ and Sγ1 DNA, but not Sγ3 DNA (Fig. 2c). Moreover, like the PKA catalytic subunit Cα (PKA-Cα), 14-3-3 bound to Sμ and Sγ1 DNA (not Sγ3 DNA) in not only *Aicda*$^{+/+}$ but also *Aicda*$^{-/-}$ B cells stimulated by LPS plus mIL-4 (Fig. 2d,e).

To determine whether 14-3-3 and AID or 14-3-3 and PKA-Cα associate on same S region DNA and in the same complex, we performed “two-step” ChIP assays using chromatin from mouse B cells stimulated by LPS plus mIL-4. Sequential ChIP with Abs to 14-3-3 and AID or Abs to AID and 14-3-3 showed that 14-3-3 and AID associated on the same Sμ and Sγ1 stretches of DNA (*Aicda*$^{-/-}$ B cells served as negative controls) (Fig. 2f). Finally, 14-3-3 and PKA-Cα associated with Sμ and Sγ1 in both *Aicda*$^{+/+}$ and *Aicda*$^{-/-}$ B cells.

Thus, 14-3-3 proteins bind to those S regions that are involved in the ongoing CSR process in an AID-independent fashion. They also show that 14-3-3 proteins are in the same complex with AID and/or PKA-Cα and on the same S region DNA.

14-3-3 proteins are upregulated in B cells undergoing CSR

We next analyzed 14-3-3 expression in germinal centers, in which B cells undergo CSR at a high rate. Like AID and BCL6, 14-3-3 proteins were expressed in human tonsil germinal centers, including the dark zone (Fig. 3a); 14-3-3 and AID, but not BCL6, showed the highest expression in the germinal center “outer zone”. Accordingly, levels of 14-3-3 and AID were upregulated in IgD$^-$ CD38$^+$ CD19$^+$ germinal center B cells, as compared to IgD$^+$ CD38$^-$ CD19$^+$ naïve B cells (Fig. 3b). Likewise, 14-3-3 proteins were highly expressed in mouse spleen germinal center areas where AID was expressed, and 14-3-3 and AID were upregulated in PNA^{hi} B220$^+$ germinal center B cells, as compared to PNA^{lo} B220$^+$ non-germinal center B cells (Fig. 3c,d).

We then analyzed the induction of 14-3-3 in B cells by stimuli that induce AID expression and CSR. Like AID, all 14-3-3 isoforms were upregulated at d 2 in mouse primary B cells stimulated by recombinant mouse CD154 (mCD154, as expressed on insect cell membrane fragments[12]) or LPS plus mIL-4 (Fig. 3e); and the upregulation of 14-3-3 and AID proteins was associated with induced levels of their respective transcripts (Fig. 3f). In human 4B6 B cells and mouse primary B cells stimulated by LPS plus mIL-4, 14-3-3 and AID localized predominantly to the cytoplasm, but were also readily detectable in the nucleus (Fig. 3g,h), where 14-3-3 formed foci (data not shown).

These experiments show that 14-3-3 proteins are upregulated in human and mouse B cells undergoing CSR *in vivo* and *in vitro*.

Blocking 14-3-3 inhibits AID recruitment to S regions and CSR

To determine whether specific blocking of 14-3-3 proteins by their high affinity inhibitor difopein (dimeric fourteen-three-three peptide inhibitor, Supplementary Fig. 3) hampers the association of 14-3-3 and AID with S region DNA and inhibits CSR, we expressed GFP–difopein fusion protein, or GFP alone as a control, in human 4B6 and 2E2 B cells by lentivirus transduction (Fig. 4a). GFP–difopein expression did not affect 14-3-3 l or AID expression (Fig. 4b), but substantially decreased binding of 14-3-3 proteins to the [5′-AGCT-3′]$_3$–24 bp oligonucleotide (Fig. 4c), and reduced the association of 14-3-3 and AID with S region DNA involved in CSR, i.e., Sμ, Sγ1 and Sα region DNA in spontaneously switching 4B6 B cells and Sμ and Sγ1 region DNA in 2E2 B cells stimulated with mAb to hCD40 plus hIL-4 (Fig. 4d).

In 4B6 B cells, blocking of 14-3-3 by difopein inhibited CSR to IgG1, IgA and IgE, as shown by reduced circle Iγ1-Cμ (69% lower), Iα-Cμ (49% lower) and Iε-Cμ (55% lower) transcripts, respectively, and reduced mature post-recombination V_HDJ_H-Cγ1 (77% lower), V_HDJ_H-Cα1 (56% lower) and V_HDJ_H-Cε (69% lower) transcripts (Fig. 5a, panel [iii] and Supplementary Fig. 4a). Likewise, blocking of 14-3-3 by difopein in 2E2 B cells stimulated with mAb to hCD40 plus hIL-4 inhibited CSR to IgG1 and IgE, as shown by reduced circle Iγ1-Cμ (48% lower) and Iε-Cμ (60% lower) transcripts and reduced mature post-recombination V_HDJ_H-Cγ1 (84% lower) and V_HDJ_H-Cε (75% lower) transcripts (Fig. 5b, panel [iii]). The reduction in circle and mature post-recombination transcripts was accompanied by decreased proportion of surface IgA^+ 4B6 B cells (Fig. 5a, panels [iv]) and $IgG1^+$ 2E2 B cells (Fig. 5b, panels [iv] and Supplementary Fig. 4b). Difopein expression, however, did not alter the number of 4B6 or 2E2 B cells throughout all 5 d of culture (Fig. 5a,b, panels [i]), the viability of those B cells (Fig. 5a,b, panels [ii]), *AICDA* expression or levels of germline I_H-C_H (Iμ-Cμ, Iγ1-Cγ1, Iα-Cα and/or Iε-Cε) or mature V_HDJ_H-Cμ transcripts (Fig. 5a,b, panels [iii]).

We next expressed GFP–difopein or GFP in purified and LPS-activated mouse primary B cells by retrovirus transduction. Blocking of 14-3-3 by GFP–difopein inhibited LPS plus mIL-4-induced CSR to IgG1 and IgE, as shown by reduced levels of circle Iγ1-Cμ and Iε-Cμ transcripts and reduced post-recombination Iμ-Cγ1 and Iμ-Cε transcripts, and decreased proportion of surface $IgG1^+$ B cells (Fig. 5c, panels [iii] and [iv], and Supplementary Fig. 4c). Decreased CSR occurred despite normal proportion, number and viability of B cells expressing GFP–difopein (Fig. 5c, panels [i] and [ii]). Likewise, difopein did not affect *Aicda* expression or levels of germline I_H-C_H or mature V_HDJ_H-Cμ transcripts (Fig. 5c, panels [iii]).

These experiments show that blocking 14-3-3 by difopein hampers binding of 14-3-3 to 5′-AGCT-3′ repeats and association of both 14-3-3 and AID with S region DNA, and inhibits CSR to IgG, IgA and IgE without decreasing AID expression, germline I_H-C_H or mature V_HDJ_H-Cμ transcripts levels or altering cell viability or proliferation.

14-3-3γ$^{-/-}$ and *14-3-3σ*$^{+/Er}$ B cells decrease AID recruitment to S regions and CSR

14-3-3γ forms homodimers and heterodimers with all other 14-3-3 isoforms except 14-3-3σ, which exists mainly as homodimer[48]. This together with the upregulation of 14-3-3γ and 14-3-3σ in switching B cells (Fig. 3) prompted us to address the role of these two isoforms in CSR using B cells deficient in 14-3-3γ (*14-3-3γ*$^{-/-}$) or expressing a C-terminally truncated 14-3-3σ protein (Er) that functions as a dominant negative (DN) mutant (*14-3-3σ*$^{+/Er}$). In *14-3-3γ*$^{-/-}$ and *14-3-3σ*$^{+/Er}$ mice, the number, proportion and viability of B220^{+} B cells and CD4^{+} and CD8^{+} T cells were normal, and so was germinal center formation (Figs. 6,7 and Supplementary Figs. 5,6).

Upon stimulation by mCD154 or LPS plus mIL-4, LPS alone, or LPS, TGF-β, mIL-4 plus dextran-conjugated mAb to IgD (anti–IgD–dextran), *14-3-3γ*$^{-/-}$ and *14-3-3σ*$^{+/Er}$ B displayed decreased CSR to IgG1, IgG3 and IgA, respectively, as compared to their wildtype B cell counterparts, without alteration in cell viability or proliferation (Figs. 6,7 and data not shown). Decreased CSR in *14-3-3γ*$^{-/-}$ and *14-3-3σ*$^{+/Er}$ B cells was associated with reduced levels of circle Iγ1-Cμ, Iγ3-Cμ, Iα-Cμ and Iε-Cμ transcripts and post-recombination Iμ-Cγ1, Iμ-Cγ3, Iμ-Cα or Iμ-Cε transcripts in spite of normal *Aicda* expression and germline I_H-C_H transcription (Fig. 6,7). Rather, reduced CSR to IgG1 in *14-3-3γ*$^{-/-}$ B cells was associated with more than 70% and 90% decreased binding of AID to Sμ and Sγ1 DNA, respectively; binding of PKA-Cα to Sμ and Sγ1 DNA was also significantly decreased, albeit at a lesser degree. Expression of the DN 14-3-3σ Er mutant also resulted in significantly decreased association of 14-3-3σ, AID and PKA-Cα with Sμ and Sγ1 DNA (Figs. 6,7).

These experiments show that at least two 14-3-3 isoforms, 14-3-3γ and 14-3-3σ, play important roles in CSR. They also show that 14-3-3γ deficiency or expression of the DN 14-3-3σ Er mutant results in reduced association of AID and PKA-Cα with S region DNA.

14-3-3 bind directly to AID through its CSR-mediating C-terminus

Having shown that 14-3-3 bound together with AID to S region DNA and played a role in enhancing/stabilizing the association of AID with S regions, we wanted to determine whether 14-3-3 adaptors interact with AID. We identified AID, but not Mre11, co-immunoprecipitating with 14-3-3 from human 4B6 B cell lysates. Also, AID with an N-terminal His_{10}–$Flag_2$ double tag interacted with endogenous 14-3-3 in 4B6 B cells (Fig. 8a). In mouse primary B cells undergoing CSR, 14-3-3 co-immunoprecipitated with AID; and this co-immunoprecipitation was not affected by extensive DNase I treatment of cell lysates before immunoprecipitation, thereby excluding the possibility that 14-3-3 and AID independently bound to DNA and co-immunoprecipitated because of DNA “bridging” (Fig. 8b).

To further prove that 14-3-3 can interact directly with AID, rather than through a third molecule, we set up a BiFC assay[49]. We divided superEYFP (sEYFP)[50] into two complementary moieties: the N-terminal 154 amino acids ($sEYFP_{1–154}$) and the C-terminal 84 amino acids ($sEYFP_{155–238}$), which were fused with Flag–tagged AID (Flag–AID–$sEYFP_{1–154}$) and influenza hemagglutinin (HA)-tagged 14-3-3 isoforms (HA–14-3-3–$sEYFP_{155–238}$), respectively. The two sEYFP moieties will complement and “give off”

strong yellow fluorescence only when juxtaposed, as a result of direct interaction between 14-3-3 and AID. By contrast, if 14-3-3 and AID interact through a third molecule, this molecule would function as a "spacer", which prevents $sEYFP_{1–154}$ and $sEYFP_{155–238}$ from complementing each other and, therefore, from giving off fluorescence (Fig. 8c). Like endogenous 14-3-3 and AID[23-26, 41] (Fig. 3g,h), HA–14-3-3ζ–$sEYFP_{155–238}$ and Flag–AID–$sEYFP_{1–154}$ localized predominantly in the cytoplasm, but were also readily detectable in the nucleus (Supplementary Fig. 7a,b). By contrast, directly associated 14-3-3ζ and AID molecules, as identified by sEYFP signal in BiFC assays involving HA–14-3-3ζ–$sEYFP_{155–238}$ and Flag–AID–$sEYFP_{1–154}$, were detectable in the cytoplasm but predominant in the nucleus (Fig. 8d and Supplementary Fig. 7c,d,e). Moreover, BiFC assays showed that 14-3-3ζ directly interacted with AID in CSR-inducible mouse CH12F3 B cells (Fig. 8e). Finally, each of the seven 14-3-3 isoforms interacted with AID, as shown by more than 40% of HeLa cells co-expressing each 14-3-3 isoform and AID being YFP^+ (Fig. 8f).

We next tested whether interaction of 14-3-3 with AID was dependent on the integrity of the AID C-terminal region, which is critical for AID to mediate CSR[23-26, 51]. BiFC assays involving 14-3-3ζ and an AID mutant lacking 9 (Flag–AIDΔ(190–198)–$sEYFP_{1–154}$) or 19 (Flag–AIDΔ(180–198)–$sEYFP_{1–154}$) C-terminal amino acids showed virtually no interaction between 14-3-3ζ and either AID mutant in HeLa cells (fewer than 3% cells being YFP^+) and mouse CH12F3 B cells (Fig. 8e,g and Supplementary Fig. 8a,b), despite the significant expression of these two AID C-terminal truncation mutants (Supplementary Fig. 8c). In contrast to the critical role of AID C-terminal region for 14-3-3/AID interaction, AID Ser38 phosphorylation is not necessary for this interaction, as a significant, albeit slightly reduced, proportion of cells were YFP^+ when co-expressing 14-3-3ζ with a S38A AID mutant (Flag–AID_{S38A}–$sEYFP_{1–154}$) (Fig. 8h), which is not phosphorylated by PKA[52]. However, BiFC assays involving 14-3-3 and PKA-Cα (Flag–PKA-Cα–$sEYFP_{1–154}$) showed that all seven 14-3-3 isoforms directly interacted with PKA-Cα in CH12F3 B cells and HeLa cells (Fig. 8e and Supplementary Fig. 8). Our BiFC assays also confirmed that difopein, which hampered AID binding to S regions, did not bind AID (Supplementary Fig. 8).

These experiments show that 14-3-3 adaptors interact with AID in switching B cells. They also show that the direct interaction of 14-3-3 and AID occurs mostly in the nucleus and depends on the integrity of the AID C-terminal region, which is critical for AID to mediate CSR.

14-3-3 proteins enhance AID-mediated DNA deamination

The above findings prompted us to investigate whether 14-3-3 can enhance AID-mediated DNA deamination. In our deamination assay, dC residues within three 5′-AGCT-3′ motifs of a 24-nt single-strand DNA oligonucleotide ($[5'\text{-AGCT-}3']_3$–24 nt) were converted to dUs by purified recombinant AID in a dose-dependent fashion, with 95% of substrate showing deamination by 20 ng of AID (Fig. 9a and Supplementary Fig. 9a,b). When added to the DNA substrate/AID reaction mixture, purified recombinant GST–14-3-3γ, GST–14-3-3σ and GST–14-3-3ζ all independently enhanced deamination of $[5'\text{-AGCT-}3']_3$–24 nt by sub-optimal amounts, from 0.5 ng to 5 ng, of AID (Fig. 9b), and did so in a dose-dependent

fashion (Supplementary Fig. 9c). Thus, 14-3-3 adaptors enhance AID-mediated DNA deamination.

Discussion

We have identified 14-3-3 proteins as adaptors specifically targeting S region DNA and recruiting AID to mediate CSR, a crucial antibody diversification process. The specificity of 14-3-3 for 5′-AGCT-3′ and the recruitment of 14-3-3 to Sμ, Sγ, Sα and Sε, all rich in 5′-AGCT-3′, emphasize the role of these adaptors in targeting the CSR machinery to the IgH locus, as possibly facilitated by high chromatin accessibility[7, 53]. Importantly, like AID, 14-3-3 proteins were efficiently induced in switching B cells and targeted selectively the upstream and downstream S regions involved in ongoing CSR events. Blocking 14-3-3 by difopein, deficiency in 14-3-3γ or expression of the DN 14-3-3σ Er mutant decreased CSR and impaired binding of AID and/or PKA-Cα to S regions, emphasizing the central role of 14-3-3 in recruiting the CSR machinery. The enhancement of AID-mediated DNA deamination by 14-3-3γ, 14-3-3σ and 14-3-3ζ, the direct interaction of AID and PKA-Cα with all 14-3-3 isoforms, and their (differential) upregulation in induced B cells suggest that multiple 14-3-3 isoforms play a role in CSR and, possibly, SHM.

Like CSR, 14-3-3 adaptors are evolutionarily conserved from frogs to humans, and so are the S region 5′-AGCT-3′ repeats, the specific 14-3-3 targets. That 14-3-3 adaptors mediate CSR through targeting 5′-AGCT-3′ provides a structural and mechanistic basis for the demonstration that the S region 5′-AGCT-3′-rich core is necessary and sufficient to mediate CSR in an evolutionary conserved fashion[37, 38]. As shown by our experiments, 14-3-3 target specifically 5′-AGCT-3′, marginally 5′-AGCA-3′ and none of the other six iterations of 5′-RGYW-3′. This is relevant to not only CSR but also SHM, as 5′-AGCT-3′ and, to a lesser extent, 5′-AGCA-3′ exist at a relatively high frequency in Ig V_H region DNA, as compared to C_H regions (Xu and Casali, unpublished). Notably, 5′-AGC[T/A]-3′ encodes for the "inherently" hypermutable Ser31 residue of the CDR1 of most human and mouse V_H gene segments[54]. The higher frequency of 5′-AGCT-3′ in S over V region DNA would underlie the far greater magnitude of lesions (DSBs) required for CSR, as compared to those (single nucleotide substitutions) required for SHM.

The highest frequency of 5′-AGCT-3′ in Sμ likely reflects the essential role of this S region in mediating direct and sequential CSR to all downstream isotypes. The higher density of 5′-AGCT-3′ repeats in human Sα1 and Sα2, rat Sγ2a and horse Sε regions, as compared to the other S regions in the same species, would likely maximize the binding "avidity" of 14-3-3 for those DNA targets. It would also possibly underpin an overall higher efficiency of CSR to and overall higher circulating levels of IgA1/IgA2 in the human, IgG2a in the rat and IgE in the horse[55-57]. As 14-3-3 proteins have been reported to bind to cruciform/stem loop structures, whose "neck" consists of two opposed and inverted 5′-AGCT-3′ motifs[46], studies are needed to address whether S region 5′-AGCT-3′ repeats indeed form cruciform and/or other secondary structures, which would enhance 14-3-3 recruitment and CSR.

Our experiments show that 14-3-3 adaptors bind specifically to S region DNA to mediate CSR. They also show that 14-3-3 proteins are in the same complex with AID on the same S

region DNA (two-step ChIP assays), and all seven 14-3-3 isoforms directly and efficiently interact with AID (BiFC assays). In spite of the predominant 14-3-3 and AID cytoplasmic localization, the interaction of 14-3-3 and AID occurred mainly in the nucleus. This is possibly due to yet to be identified nucleus-specific regulation and/or modifications of 14-3-3[40] and/or AID[58], and likely contributes to stabilization and/or retention of AID in the nucleus[22-26]. That 14-3-3 adaptors are the AID-binding "co-factors" necessary for CSR is indicated by our demonstration that 14-3-3 proteins do not bind AIDΔ(190–198), the C-terminal truncation AID mutant that cannot mediate CSR in spite of its full DNA deamination activity[23-26, 51]. The dependence of both AID stability and CSR on the integrity of the 14-3-3-interacting C-terminal region of AID strongly suggests that these adaptors regulate both processes. As we show, 14-3-3 proteins enhance AID-mediated DNA deamination to a degree comparable to that of an AID upmutant, which was more effective in inducing CSR than wildtype AID[27]. 14-3-3 may enhance the intrinsic AID enzymatic activity through induction of conformational changes and/or AID association with DNA.

Our findings outline an important role of 14-3-3 proteins in the antibody response. As we show, expression of 14-3-3 adaptors is upregulated by the stimuli that also induce AID expression and CSR and in the same B lymphocyte stage-specific fashion, thereby defining a precise window for CSR to occur. 14-3-3 execute diverse adaptor functions through induction of conformational changes and/or scaffolding of different ligands/client proteins[40]. The direct interaction of 14-3-3 with the AID_{S38A} mutant indicates that AID Ser38 phosphorylation by PKA is dispensable for 14-3-3/AID interaction (KRRDpS_{38}AT of AID is not a putative 14-3-3-binding motif[59]) and 14-3-3-mediated recruitment/stabilization of AID to S regions[52]. PKA does not directly bind to DNA, but associates with S regions in switching B cells[52], possibly through 14-3-3, as suggested by the decreased binding of PKA-Cα to S region DNA in *14-3-3*$\gamma^{-/-}$ and *14-3-3*$\sigma^{+/Er}$ B cells. 14-3-3 proteins were in a complex with PKA-Cα on S region DNA involved in an ongoing CSR and would recruit PKA to S regions by direct interaction with PKA-Cα and/or indirectly through A kinase-anchoring proteins (AKAPs)[52, 60]. 14-3-3, however, may also contribute to the overall CSR process in other ways.

14-3-3 adaptors play important roles in vital cellular processes by integrating extracellular signaling cues[41]. Deficiency or impairment of a single 14-3-3 isoform would have no significant negative impact on basic lymphocyte functions, as suggested by our finding that 14-3-3γ deficiency or expression of the 14-3-3σ Er DN mutant allowed for normal B and T cell development, germinal center formation and B cell proliferation and survival, as likely mediated by the total basal 14-3-3 pool. However, basal levels of the 14-3-3 pool are likely insufficient to maintain cell survival and proliferative response in the presence of significant DNA damage[61]. Overcoming such limitations likely requires higher levels of most or all 14-3-3 isoforms. Likewise, higher 14-3-3 levels are required for efficient targeting of the CSR machinery. These higher requirements would be met by the marked upregulation of 14-3-3 adaptors in B cells undergoing CSR. Further studies are needed to outline the precise role of 14-3-3 proteins, and possibly their post-translational modifications, e.g., phosphorylation[48], in targeting AID to the Ig locus and, perhaps, to other loci, such as the *BCL6* and *c-Myc* proto-oncogenes, in AID-mediated B cell lymphomagenesis[62-64].

Methods

AID-mediated DNA deamination

Purified recombinant GST–AID was incubated with 1 pmole HPLC-purified single-strand [5′-AGCT-3′]$_3$–24 nt oligonucleotide (5′-AGCTAAAAAGCTAAAAAGCTAAAA-3′, labeled with Alexa Fluor 647 at the 5′ end) in a 20 μl reaction mixture containing 25 mM Tris–HCl (pH 7.5), 50 mM NaCl, 0.5 mM DTT, 0.01% CHAPS, 1 mM GSH, 200 ng RNase A (Qiagen) and 0.2 unit Ung (New England Biolabs, to convert dU to abasic sites) for 30 m at 37°C. The reaction was followed by cleavage of heat-labile abasic sites by heating at 95°C for 10 m in the presence of 200 mM NaOH. The intact substrate and cleavage products were fractionated in denaturing 15% PAGE containing 8 M urea and visualized using a Typhoon™ 9410 scanner (GE Healthcare). The intensity of substrate and cleavage product bands was quantified by ImageQuant™ TL software (GE Healthcare).

Affinity purification and identification (MudPIT) of 5′-AGCT-3′-binding proteins

The biotinylated double-strand [5′-AGCT-3′]$_3$–24 bp oligonucleotide was immobilized on NeutrAvidin-conjugated agarose beads following manufacturer's instructions (Pierce Biotechnology). Nuclear extract proteins were prepared from 2×10^9 human IgM$^+$ IgD$^+$ 4B6 B cells in buffer (20 mM HEPES, pH 7.9, 320 mM KCl, 5 mM $MgCl_2$) with protease inhibitors (Sigma-Aldrich Co.), as we described[12, 65, 66]. After dilution in 40 ml of binding buffer (20 mM HEPES, pH 7.9, 150 mM KCl, 4 mM $MgCl_2$, 1 mM EDTA, 0.05% NP-40), nuclear extract proteins were mixed with 1 ml of NeutrAvidin beads bearing the [5′-AGCT-3′]$_3$–24 bp oligonucleotide in the presence of a 100-fold molar excess of [3′-AGCT-5′]$_3$–24 bp oligonucleotide and 100 μg ml^{-1} poly(dI/dC) for 2 h at 25°C. After centrifugation, the pelleted beads were resuspended in washing buffer (20 mM HEPES, pH 7.9, 200 mM KCl, 0.05% NP-40) and transferred into a 10 ml polystyrene column (Pierce Biotechnology). After washing with 100 ml of the washing buffer, bound proteins were eluted by 15 ml of elution buffer (20 mM HEPES, pH 7.9, 600 mM NaCl, 0.05% NP-40) and collected in 1-ml fractions. MudPIT analysis to identify eluted proteins was performed as described[67] (detailed in Supplementary Methods).

B cells and *in vitro* CSR

Spontaneous switching human IgM$^+$ IgD$^+$ 4B6 B cells, inducible switching human IgM$^+$ IgD$^+$ 2E2 B cells and inducible switching mouse IgM$^+$ CH12F3 B cells were as we described[12]. Human IgD$^-$ CD38$^+$ CD19$^+$ germinal center B cells and IgD$^+$ CD38$^-$ CD19$^+$ naïve B cells from tonsil and mouse B220$^+$ primary B cells were prepared as we described[12, 68]. To analyze spontaneous CSR in human 4B6 B cells, IgG$^-$ IgA$^-$ cells were cultured at 5×10^4 cell ml^{-1} in RPMI-1640 medium (Invitrogen Corp.) supplemented with 10% fetal calf serum (Hyclone) and 1% penicillin-streptomycin (FCS-RPMI). To induce CSR to IgG1, human 2E2 B cells were cultured at 5×10^4 cell ml^{-1} and stimulated with agonistic mAb to hCD40 (IgG1 mAb G28-5, ATCC) plus recombinant hIL-4 (Genzyme Co.) for 4 d. Mouse B cells were labeled with CFSE (Invitrogen) and induced to undergo CSR by mCD154 or LPS (*E. coli* serotype 055:B5; Sigma-Aldrich Co.) plus appropriate cytokines, as we reported[12]. All protocols involving human tissues and/or cells were in accordance to the rules and regulations of the IRB of UC Irvine.

B cell transduction by lentivirus (human) or retrovirus (mouse)

The coding sequence for GFP or GFP–difopein was cloned into the lentiviral vector pFUW[69] to construct pFUW–GFP or pFUW–GFP–difopein vector, which was then co-transfected with packaging plasmids pREV, pRRE and pVSV-G into HEK-293T cells using Pro-Fection® Mammalian Transfection System (Promega) to generate lentivirus pseudo-typed with VSV-G. For transduction, viruses in culture supernatants were cleared from cells by filtration through 0.45 μm filters and incubated with 10^5 human B cells in the presence of 6 μg ml^{-1} polybrene (Sigma-Aldrich Co.). After 24 h, culture media were replaced with virus-free medium. After 72 h, GFP^+ cells were sorted, resulting in over 90% of B cells stably expressing GFP or GFP–difopein. To construct pTAC–GFP or pTAC–GFP–difopein retroviral vector, the coding sequence for GFP or GFP–difopein was cloned into the retroviral vector pCSretTAC. Generation of retroviruses, transduction of purified and LPS-activated mouse B cells and CSR analysis were as we described[12].

BiFC

To express HA–14-3-3ζ–$sEYFP_{155–238}$ and Flag–AID–$sEYFP_{1–154}$ (sEYFP is an EYFP variant that gives off three times of fluorescence per molecule than EYFP[50]), CSR-inducible mouse CH12F3 B cells (10^7) were mixed gently with 10 μg of each plasmid in 800 μl RPMI1640 and then electroporated at 250 volts and 900 Ω in a Gene Pulser II (BioRad). After incubation in 2 ml of FCS-RPMI and stimulated by LPS, mIL-4 plus TGF-β for 16 to 24 h, CH12F3 B cells were analyzed for fluorescent intensities using a Gemini XPS microplate spectrofluorometer (MDS Analytical Technologies). To express HA–14-3-3ζ–$sEYFP_{155–238}$ and Flag–AID–$sEYFP_{1–154}$ proteins in HeLa cells, 5×10^5 HeLa cells were transfected with 1 μg of each plasmid using Lipofectamine™ (Invitrogen Corp.). Cells were stained with 7–AAD 24 h after transfection and analyzed by flow cytometry; 36 h after transfection, cells were stained with DAPI, and images were captured using an Axiovert microscope (Carl Zeiss Microimaging).

ChIP assays

ChIP assays were performed as we described[12, 66, 70] (detailed in Supplementary Methods). Two-step ChIP assays were performed as follows. Crosslinked protein/DNA complexes were immunoprecipitated by the first Ab and captured by protein G agarose beads. After washing and centrifugation, the beads were pelleted and the supernatant discarded. The pelleted beads were resuspended in 40 μl freshly made Re-ChIP buffer (16.7 mM Tris–HCl, pH 8.0, 167 mM NaCl, 1.2 mM EDTA, 1.1% Triton X-100, 10 mM DTT and protease inhibitors) and incubated for 30 m at 25°C. The supernatant (40 μl) was saved and diluted with 1.6 ml buffer (16.7 mM Tris–HCl, pH 8.0, 167 mM NaCl, 1.2 mM EDTA, 1.1% Triton X-100) supplemented with 100 μg purified salmon sperm DNA, 100 μg purified yeast tRNA (Invitrogen Corp.) and 1 mg purified BSA (New England Biolabs) and precipitated by the second Ab. The procedures following the second immunoprecipitation, including binding to agarose beads bearing protein G, reverse crosslinking and DNA purification, were the same as those of ChIP assays.

Mice

14-3-3γ$^{-/-}$ mice, originally generated on the 129 genetic background[42], were backcrossed onto the C57BL/6 background for 6 generations. *14-3-3γ*$^{-/-}$ mice were born at the Mendelian ratio, and at the age of 8-12 weeks, they were normal in appearance, size and weight, and were fertile. Heterozygotic *14-3-3σ*$^{+/Er}$ mice (*14-3-3σ*$^{Er/Er}$ mice die *in utero*), originally on the FVB genetic background[71], were backcrossed onto the C57BL/6 background for 9 generations. At the age of 8-12 weeks, *14-3-3σ*$^{+/Er}$ mice displayed a repeated epilation (Er) phenotype, as reported for *14-3-3σ*$^{+/Er}$ mice on the FVB genetic background[71], but were normal in size and weight, and were fertile. Mice used in all experiments were 8-12 weeks. All mice were maintained in the pathogen-free barrier vivarium at UC Irvine. All protocols were in accordance to the rules and regulations of the IACUC of UC Irvine.

Statistical analysis

The Prism software was used for the paired t-test to analyze significance of differences, and *p* values less than 0.05 were considered significant.

Supplementary Material

Refer to Web version on PubMed Central for supplementary material.

Acknowledgments

Dr. A. Muslin (Washington University, St. Louis) and Dr. A. Wynshaw-Boris (University of California, San Francisco) for advice; I. McLeod (Scripps Research Institute) for performing MudPIT; Dr. H. Hermeking and Dr. D. Lodygin (Ludwig–Maximilians–University, Munich) for sharing preliminary data on 14-3-3σ; Dr. J. S. Hawkins and Mr. M. Crabtree for transcripts analysis; P. Patel, A. Bui and S. Yao for technical assistance; Dr. L. Yang and Dr. D. Baltimore (Caltech, Pasadena) for the pFUW lentiviral constructs and Dr. C. Murre (University of California, San Diego) for the pTAC retroviral construct; Dr. F. Byrne and Dr. R. Kurzeja (Amgen Inc.) for the purified recombinant AID; Dr. Y. Du for the purified recombinant 14-3-3 proteins; the UC Irvine Pathology Research Core Facility for immunohistochemistry. S.-R.P. was a fellow of the Korea Research Foundation. H. F. is a Georgia Cancer Coalition Distinguished Cancer Scholar and a Georgia Research Alliance Distinguished Investigator. P. C. is the Donald L. Bren Professor of Medicine, Molecular Biology and Biochemistry. H. F. was supported by the NIH grant P01 CA 116676. J. R. Y. III was supported by the NIH grant P41 RR011823. This work was supported by the NIH grants AI 045011, AI 079705 and AI 060573 to P.C.

References

1. Maizels N. Immunoglobulin gene diversification. Annu Rev Genet. 2005; 39:23–46. [PubMed: 16285851]
2. Casali, P. Somatic recombination and hypermutation in the immune system. In: Krebs, JE.; Goldstein, ES.; Kilpatrick, ST., editors. Lewin's Genes X. Jones & Bartlett; Sudbury, MA: 2011. p. 570-623.
3. Odegard VH, Schatz DG. Targeting of somatic hypermutation. Nat Rev Immunol. 2006; 6:573–583. [PubMed: 16868548]
4. Casali P, Pal Z, Xu Z, Zan H. DNA repair in antibody somatic hypermutation. Trends Immunol. 2006; 27:313–321. [PubMed: 16737852]
5. Teng G, Papavasiliou FN. Immunoglobulin somatic hypermutation. Annu Rev Genet. 2007; 41:107–120. [PubMed: 17576170]
6. Peled JU, et al. The biochemistry of somatic hypermutation. Annu Rev Immunol. 2008; 26:481–511. [PubMed: 18304001]

7. Stavnezer J, Guikema JE, Schrader CE. Mechanism and regulation of class switch recombination. Annu Rev Immunol. 2008; 26:261–292. [PubMed: 18370922]
8. Xu W, et al. Viral double-stranded RNA triggers Ig class switching by activating upper respiratory mucosa B cells through an innate TLR3 pathway involving BAFF. J Immunol. 2008; 181:276–287. [PubMed: 18566393]
9. Pone EJ, et al. Toll-like receptors and B-cell receptors synergize to induce immunoglobulin class-switch DNA recombination: relevance to microbial antibody responses. Crit Rev Immunol. 2010; 30:1–29. [PubMed: 20370617]
10. Muramatsu M, Nagaoka H, Shinkura R, Begum NA, Honjo T. Discovery of activation-induced cytidine deaminase, the engraver of antibody memory. Adv Immunol. 2007; 94:1–36. [PubMed: 17560270]
11. Delker RK, Fugmann SD, Papavasiliou FN. A coming-of-age story: activation-induced cytidine deaminase turns 10. Nat Immunol. 2009; 10:1147–1153. [PubMed: 19841648]
12. Park SR, et al. HoxC4 binds to the promoter of the cytidine deaminase AID gene to induce AID expression, class-switch DNA recombination and somatic hypermutation. Nat Immunol. 2009; 10:540–550. [PubMed: 19363484]
13. Conticello SG, Langlois MA, Neuberger MS. Insights into DNA deaminases. Nat Struct Mol Biol. 2007; 14:7–9. [PubMed: 17203067]
14. Chelico L, Pham P, Calabrese P, Goodman MF. APOBEC3G DNA deaminase acts processively 3′ → 5′ on single-stranded DNA. Nat Struct Mol Biol. 2006; 13:392–399. [PubMed: 16622407]
15. Nowarski R, Britan-Rosich E, Shiloach T, Kotler M. Hypermutation by intersegmental transfer of APOBEC3G cytidine deaminase. Nat Struct Mol Biol. 2008; 15:1059–1066. [PubMed: 18820687]
16. Pham P, Bransteitter R, Petruska J, Goodman MF. Processive AID-catalysed cytosine deamination on single-stranded DNA simulates somatic hypermutation. Nature. 2003; 424:103–107. [PubMed: 12819663]
17. Larijani M, et al. AID associates with single-stranded DNA with high affinity and a long complex half-life in a sequence-independent manner. Mol Cell Biol. 2007; 27:20–30. [PubMed: 17060445]
18. Chaudhuri J, Khuong C, Alt FW. Replication protein A interacts with AID to promote deamination of somatic hypermutation targets. Nature. 2004; 430:992–998. [PubMed: 15273694]
19. Xu Z, et al. Regulation of *aicda* expression and AID activity: relevance to somatic hypermutation and class switch DNA recombination. Crit Rev Immunol. 2007; 27:367–397. [PubMed: 18197815]
20. Crouch EE, et al. Regulation of AID expression in the immune response. J Exp Med. 2007; 204:1145–1156. [PubMed: 17452520]
21. Zan H, et al. Lupus-prone MRL/$Fas^{lpr/lpr}$ mice display increased AID expression and extensive DNA lesions, comprising deletions and insertions, in the immunoglobulin locus: concurrent upregulation of somatic hypermutation and class switch DNA recombination. Autoimmunity. 2009; 42:89–103. [PubMed: 19156553]
22. Aoufouchi S, et al. Proteasomal degradation restricts the nuclear lifespan of AID. J Exp Med. 2008; 205:1357–1368. [PubMed: 18474627]
23. Geisberger R, Rada C, Neuberger MS. The stability of AID and its function in class-switching are critically sensitive to the identity of its nuclear-export sequence. Proc Natl Acad Sci USA. 2009; 106:6736–6741. [PubMed: 19351893]
24. Ito S, et al. Activation-induced cytidine deaminase shuttles between nucleus and cytoplasm like apolipoprotein B mRNA editing catalytic polypeptide 1. Proc Natl Acad Sci USA. 2004; 101:1975–1980. [PubMed: 14769937]
25. McBride KM, Barreto V, Ramiro AR, Stavropoulos P, Nussenzweig MC. Somatic hypermutation is limited by CRM1-dependent nuclear export of activation-induced deaminase. J Exp Med. 2004; 199:1235–1244. [PubMed: 15117971]
26. Patenaude AM, et al. Active nuclear import and cytoplasmic retention of activation-induced deaminase. Nat Struct Mol Biol. 2009; 16:517–527. [PubMed: 19412186]
27. Wang M, Yang Z, Rada C, Neuberger MS. AID upmutants isolated using a high-throughput screen highlight the immunity/cancer balance limiting DNA deaminase activity. Nat Struct Mol Biol. 2009; 16:769–776. [PubMed: 19543289]

28. Schrader CE, Linehan EK, Mochegova SN, Woodland RT, Stavnezer J. Inducible DNA breaks in Ig S regions are dependent on AID and UNG. J Exp Med. 2005; 202:561–568. [PubMed: 16103411]
29. Zan H, Casali P. AID- and Ung-dependent generation of staggered double-strand DNA breaks in immunoglobulin class switch DNA recombination: a post-cleavage role for AID. Mol Immunol. 2008; 46:45–61. [PubMed: 18760480]
30. Rada C, Di Noia JM, Neuberger MS. Mismatch recognition and uracil excision provide complementary paths to both Ig switching and the A/T-focused phase of somatic mutation. Mol Cell. 2004; 16:163–171. [PubMed: 15494304]
31. Larson ED, Cummings WJ, Bednarski DW, Maizels N. MRE11/RAD50 cleaves DNA in the AID/UNG-dependent pathway of immunoglobulin gene diversification. Mol Cell. 2005; 20:367–375. [PubMed: 16285919]
32. Yan CT, et al. IgH class switching and translocations use a robust non-classical end-joining pathway. Nature. 2007; 449:478–482. [PubMed: 17713479]
33. Dinkelmann M, et al. Multiple functions of MRN in end-joining pathways during isotype class switching. Nat Struct Mol Biol. 2009; 16:808–813. [PubMed: 19633670]
34. Dunnick W, Hertz GZ, Scappino L, Gritzmacher C. DNA sequences at immunoglobulin switch region recombination sites. Nucleic Acids Res. 1993; 21:365–372. [PubMed: 8441648]
35. Ehrenstein MR, Neuberger MS. Deficiency in Msh2 affects the efficiency and local sequence specificity of immunoglobulin class-switch recombination: parallels with somatic hypermutation. EMBO J. 1999; 18:3484–3490. [PubMed: 10369687]
36. Wu X, et al. A role for the MutL mismatch repair Mlh3 protein in immunoglobulin class switch DNA recombination and somatic hypermutation. J Immunol. 2006; 176:5426–5437. [PubMed: 16622010]
37. Zarrin AA, et al. An evolutionarily conserved target motif for immunoglobulin class-switch recombination. Nat Immunol. 2004; 5:1275–1281. [PubMed: 15531884]
38. Luby TM, Schrader CE, Stavnezer J, Selsing E. The μ switch region tandem repeats are important, but not required, for antibody class switch recombination. J Exp Med. 2001; 193:159–168. [PubMed: 11148220]
39. Zarrin AA, Goff PH, Senger K, Alt FW. Sγ3 switch sequences function in place of endogenous Sγ1 to mediate antibody class switching. J Exp Med. 2008; 205:1567–1572. [PubMed: 18541713]
40. Fu H, Subramanian RR, Masters SC. 14-3-3 proteins: structure, function, and regulation. Annu Rev Pharmacol Toxicol. 2000; 40:617–647. [PubMed: 10836149]
41. Morrison DK. The 14-3-3 proteins: integrators of diverse signaling cues that impact cell fate and cancer development. Trends Cell Biol. 2009; 19:16–23. [PubMed: 19027299]
42. Steinacker P, et al. Unchanged survival rates of 14-3-3γ knockout mice after inoculation with pathological prion protein. Mol Cell Biol. 2005; 25:1339–1346. [PubMed: 15684385]
43. Chan TA, Hermeking H, Lengauer C, Kinzler KW, Vogelstein B. 14-3-3σ is required to prevent mitotic catastrophe after DNA damage. Nature. 1999; 401:616–620. [PubMed: 10524633]
44. Zan H, et al. The translesion DNA polymerase ζ plays a major role in Ig and bcl-6 somatic hypermutation. Immunity. 2001; 14:643–653. [PubMed: 11371365]
45. Wang H, Zhang L, Liddington R, Fu H. Mutations in the hydrophobic surface of an amphipathic groove of 14-3-3ζ disrupt its interaction with Raf-1 kinase. J Biol Chem. 1998; 273:16297–16304. [PubMed: 9632690]
46. Zannis-Hadjopoulos M, Yahyaoui W, Callejo M. 14-3-3 cruciform-binding proteins as regulators of eukaryotic DNA replication. Trends Biochem Sci. 2008; 33:44–50. [PubMed: 18054234]
47. Nakamura M, et al. High frequency class switching of an IgM^+ B lymphoma clone CH12F3 to IgA^+ cells. Int Immunol. 1996; 8:193–201. [PubMed: 8671604]
48. Aitken A, et al. Specificity of 14-3-3 isoform dimer interactions and phosphorylation. Biochem Soc Trans. 2002; 30:351–360. [PubMed: 12196094]
49. Hu CD, Chinenov Y, Kerppola TK. Visualization of interactions among bZIP and Rel family proteins in living cells using bimolecular fluorescence complementation. Mol Cell. 2002; 9:789–798. [PubMed: 11983170]

50. Nagai T, et al. A variant of yellow fluorescent protein with fast and efficient maturation for cell-biological applications. Nat Biotechnol. 2002; 20:87–90. [PubMed: 11753368]
51. Barreto V, Reina-San-Martin B, Ramiro AR, McBride KM, Nussenzweig MC. C-terminal deletion of AID uncouples class switch recombination from somatic hypermutation and gene conversion. Mol Cell. 2003; 12:501–508. [PubMed: 14536088]
52. Vuong BQ, et al. Specific recruitment of protein kinase A to the immunoglobulin locus regulates class-switch recombination. Nat Immunol. 2009; 10:420–426. [PubMed: 19234474]
53. Wang L, Wuerffel R, Feldman S, Khamlichi AA, Kenter AL. S region sequence, RNA polymerase II, and histone modifications create chromatin accessibility during class switch recombination. J Exp Med. 2009; 206:1817–1830. [PubMed: 19596805]
54. Chang B, Casali P. The CDR1 sequences of a major proportion of human germline Ig VH genes are inherently susceptible to amino acid replacement. Trends Immunol. 1994; 15:367–373.
55. Pascual DW, Coste M, Boyaka PN, Kiyono H, McGhee JR. Spontaneously hypertensive rat: cholera toxin converts suppression to immunity through a Th2 cell-IL-4 pathway. Am J Physiol. 1997; 273:R1509–1518. [PubMed: 9362318]
56. Cunningham-Rundles C. Physiology of IgA and IgA deficiency. J Clin Immunol. 2001; 21:303–309. [PubMed: 11720003]
57. Wagner B. IgE in horses: occurrence in health and disease. Vet Immunol Immunopathol. 2009; 132:21–30. [PubMed: 19819562]
58. Ordinario EC, Yabuki M, Larson RP, Maizels N. Temporal regulation of Ig gene diversification revealed by single-cell imaging. J Immunol. 2009; 183:4545–4553. [PubMed: 19748985]
59. Yaffe MB, et al. The structural basis for 14-3-3:phosphopeptide binding specificity. Cell. 1997; 91:961–971. [PubMed: 9428519]
60. Diviani D, Abuin L, Cotecchia S, Pansier L. Anchoring of both PKA and 14-3-3 inhibits the Rho-GEF activity of the AKAP-Lbc signaling complex. EMBO J. 2004; 23:2811–2820. [PubMed: 15229649]
61. Mohammad DH, Yaffe MB. 14-3-3 proteins, FHA domains and BRCT domains in the DNA damage response. DNA Repair (Amst). 2009; 8:1009–1017. [PubMed: 19481982]
62. Pasqualucci L, et al. AID is required for germinal center-derived lymphomagenesis. Nat Genet. 2008; 40:108–112. [PubMed: 18066064]
63. Okazaki IM, Kotani A, Honjo T. Role of AID in tumorigenesis. Adv Immunol. 2007; 94:245–273. [PubMed: 17560277]
64. Liu M, Schatz DG. Balancing AID and DNA repair during somatic hypermutation. Trends Immunol. 2009; 30:173–181. [PubMed: 19303358]
65. Schaffer A, et al. Selective inhibition of class switching to IgG and IgE by recruitment of the HoxC4 and Oct-1 homeodomain proteins and Ku70/Ku86 to newly identified ATTT *cis*-elements. J Biol Chem. 2003; 278:23141–23150. [PubMed: 12672812]
66. Kim EC, Edmonston CR, Wu X, Schaffer A, Casali P. The HoxC4 homeodomain protein mediates activation of the immunoglobulin heavy chain 3′ hs1,2 enhancer in human B cells. Relevance to class switch DNA recombination. J Biol Chem. 2004; 279:42258–42269. [PubMed: 15252056]
67. Lu B, Xu T, Park SK, Yates JRr. Shotgun protein identification and quantification by mass spectrometry. Methods Mol Biol. 2009; 564:261–288. [PubMed: 19544028]
68. Zan H, et al. The translesion DNA polymerase θ plays a dominant role in immunoglobulin gene somatic hypermutation. EMBO J. 2005; 24:3757–3769. [PubMed: 16222339]
69. Lois C, Hong EJ, Pease S, Brown EJ, Baltimore D. Germline transmission and tissue-specific expression of transgenes delivered by lentiviral vectors. Science. 2002; 295:868–872. [PubMed: 11786607]
70. Zan H, Wu X, Komori A, Holloman WK, Casali P. AID-dependent generation of resected double-strand DNA breaks and recruitment of Rad52/Rad51 in somatic hypermutation. Immunity. 2003; 18:727–738. [PubMed: 12818155]
71. Herron BJ, et al. A mutation in stratifin is responsible for the repeated epilation (Er) phenotype in mice. Nat Genet. 2005; 37:1210–1212. [PubMed: 16200063]

Abbreviations used in this paper

Ab	antibody
AID	activation-induced cytidine deaminase
BiFC assay	bimolecular fluorescence complementation assay
ChIP	chromatin immunoprecipitation
Co-IP	co-immunoprecipitation
CSR	class switch DNA recombination
difopein	dimeric fourteen-three-three peptide inhibitor
DSB	double-strand DNA break
EMSA	electrophoretic mobility shift assay
Er	repeated epilation
Ig	immunoglobulin
MudPIT	multiple dimensional protein identification technology
NHEJ	non-homologous recombination
SHM	somatic hypermutation

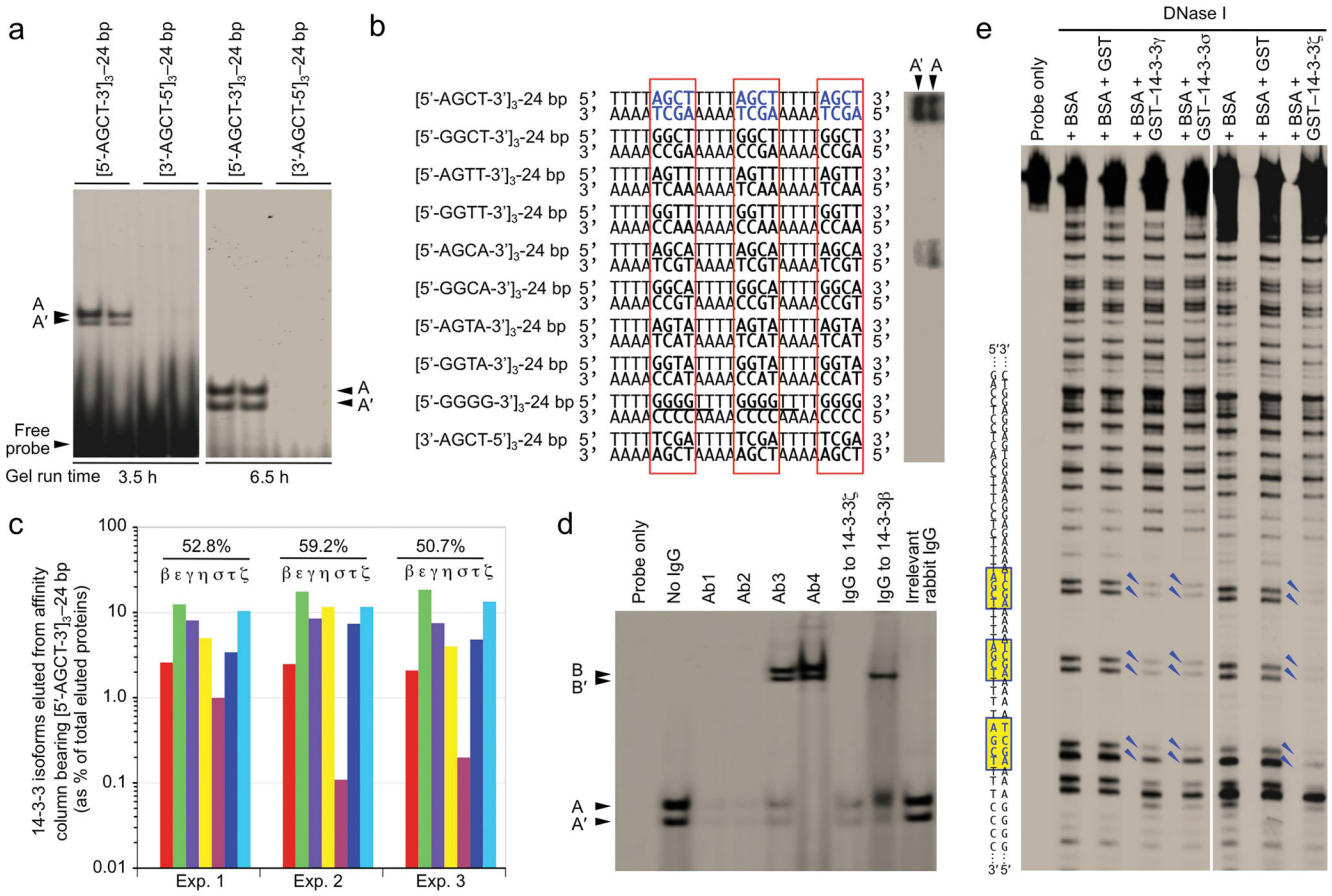

Figure 1.

14-3-3 proteins bind to 5′-AGCT-3′ repeats. (**a**) EMSA with nuclear extracts from spontaneously switching human 4B6 B cells and the [5′-AGCT-3′]$_3$–24 bp or the control [3′-AGCT-5′]$_3$–24 bp oligonucleotide probe. Duplicate samples were separated in a 7% native PAGE gel for 3.5 h (left panel) or 6.5 h (right panel, free probes ran off the gel). (**b**) EMSA with 4B6 B cell nuclear extracts and the [5′-AGCT-3′]$_3$–24 bp oligonucleotide probe or oligonucleotide probes containing three repeats of the other seven iterations of 5′-RGYW-3′, 5′-GGGG-3′ (5′-GGGG-3′ is part of 5′-GGGGT-3′, as underlined) or 3′-AGCT-5′. (**c**) Relative amount of each of the seven 14-3-3 isoforms in the total proteins eluted from the [5′-AGCT-3′]$_3$–24 bp oligonucleotide affinity column in three independent experiments (MudPIT analysis). The combined amounts of the seven 14-3-3 isoforms are indicated. (**d**) 14-3-3 proteins were present in complexes containing B cell nuclear extract proteins and the [5′-AGCT-3′]$_3$–24 bp oligonucleotide probe. Abs recognizing all 14-3-3 isoforms (Ab1, ab6081; Ab2, sc-629; Ab3, sc-13959; Ab4, ab9063) or specific isoforms (14-3-3ζ or -β) blocked formation of the A and/or A′ complexes or shifted them to form B and/or B′. (**e**) Footprint showing protection from DNase I digestion of the three 5′-AGCT-3′ motifs (highlighted in yellow) in the 126-bp oligonucleotide by GST–14-3-3γ, GST–14-3-3σ or GST–14-3-3ζ, but not BSA or BSA plus GST (arrowheads indicate protected dG and dC).

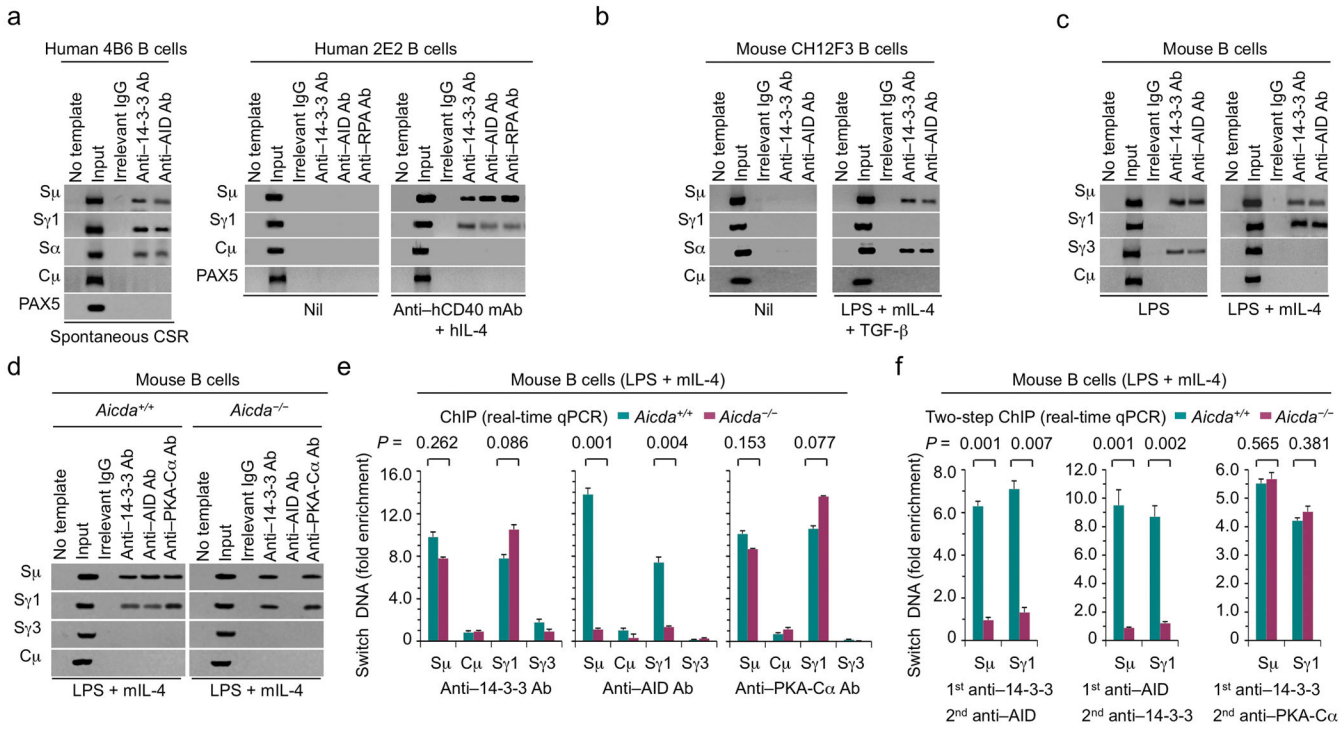

Figure 2.

14-3-3 adaptors bind to the S regions involved in ongoing CSR. (**a**) ChIP assays involving chromatin from human IgM$^+$ IgD$^+$ 4B6 B cells and Ab to 14-3-3 or AID, and specifying Sμ, Sγ1, Sα (Sα1/Sα2), Cμ and *PAX5* DNA (left); or chromatin from human 2E2 B cells stimulated by nil or mAb to hCD40 plus hIL-4, and specifying Sμ, Sγ1, Cμ and *PAX5* DNA precipitated by Ab to 14-3-3, AID or RPA (right). (**b,c**) ChIP assays involving chromatin from mouse IgM$^+$ CH12F3 B cells stimulated by nil or LPS, mIL-4 plus TGF-β and specifying Sμ, Sγ1, Sα and Cμ DNA (**b**), or chromatin from mouse primary B cells (B220$^+$) stimulated by LPS or LPS plus mIL-4 and specifying Sμ, Sγ1, Sγ3 and Cμ DNA (**c**), precipitated by Ab to 14-3-3 or AID. (**d,e**) ChIP assays involving chromatin from *Aicda*$^{+/+}$ and *Aicda*$^{-/-}$ mouse B cells stimulated by LPS plus mIL-4 and Ab to 14-3-3, AID or PKA-Cα, and specifying (**d**) and quantifying Sμ, Sγ1, Sγ3 and Cμ DNA (**e**, data expressed as "fold enrichment" over DNA precipitated by irrelevant IgG, mean and s.d. of triplicate samples). (**f**) Two-step ChIP assays involving chromatin from *Aicda*$^{+/+}$ and *Aicda*$^{-/-}$ mouse B cells stimulated by LPS plus mIL-4 and sequential precipitation by Abs to 14-3-3 and AID (left), or Abs to AID and 14-3-3 (middle), or Abs to 14-3-3 and PKA-Cα (right). Quantified Sμ and Sγ1 DNA are expressed as fold enrichment over DNA precipitated by irrelevant IgG used in the second immunoprecipitation step (mean and s.d. of triplicate samples).

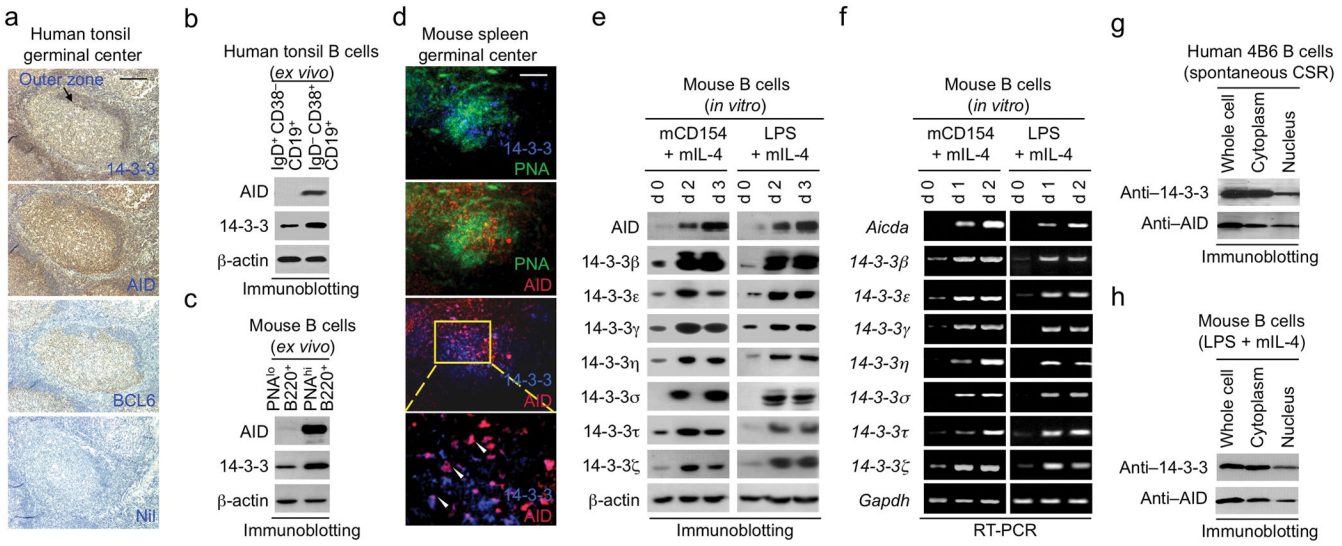

Figure 3.

14-3-3 proteins are upregulated in germinal center B cells and in B cells undergoing CSR *in vitro*. (**a**) Immunohistochemistry of serial human tonsil sections stained with Ab to 14-3-3, AID or BCL6 (brown signals) or no Ab ("Nil", showing blue signals from the hematoxylin counterstaining). Scale bar: 50 μm. (**b**) Expression of AID and 14-3-3 in sorted tonsil IgD^+ $CD38^-$ $CD19^+$ naive and IgD^- $CD38^+$ $CD19^+$ germinal center B cells. (**c**) Expression of AID and 14-3-3 in sorted spleen PNA^{lo} $B220^+$ non-germinal center B cells and PNA^{hi} $B220^+$ germinal center B cells from NP_{16}–CGG-immunized C57BL/6 mice. (**d**) Expression of 14-3-3 and AID in germinal centers (green, as stained by FITC-conjugated PNA) in serial spleen sections of C57BL/6 mice immunized with NP_{16}–CGG for 7 d (one representative of four experiments). The magnified yellow-boxed area shows co-expression of 14-3-3 and AID in germinal center B cells (3 representative cells are indicated by arrowheads). Scale bar: 50 μm. (**e,f**) Immunoblotting (**e**) and RT-PCR (**f**) analysis of AID and the seven 14-3-3 isoforms in freshly isolated mouse primary B cells (d 0) or B cells after stimulation by mCD154 or LPS plus mIL-4. (**g** and **h**) Expression of 14-3-3 and AID in the whole cell, cytoplasm and nucleus of human 4B6 B cells (**g**) and mouse primary B cells stimulated by LPS plus mIL-4 for 60 h (**h**).

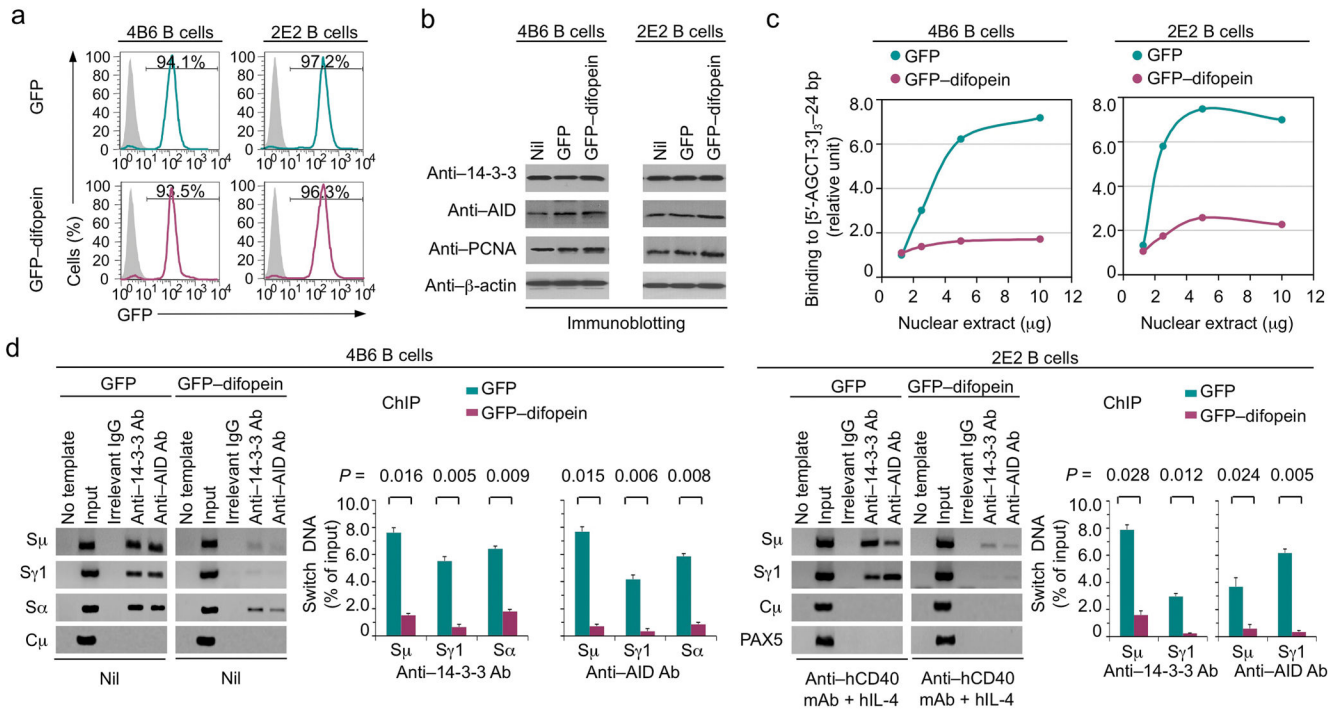

Figure 4.

Blocking 14-3-3 by difopein inhibits 14-3-3 binding to 5′-AGCT-3′ repeats and hampers the binding of 14-3-3 and AID to S regions. (**a**) Flow cytometry analysis of the proportion (GFP^+) of human 4B6 and 2E2 B cells expressing nil (gray shade), or GFP or GFP–difopein by lentivirus transduction. (**b**) Expression of 14-3-3 (all isoforms), AID and PCNA in 4B6 B cells and in mAb to hCD40 plus hIL-4-stimulated 2E2 B cells expressing nil, or GFP or GFP–difopein. (**c**) EMSA analysis of the binding to the $[5′\text{-AGCT-}3′]_3$–24 bp oligonucleotide by two-fold increasing amounts of nuclear extracts from 4B6 B cells and mAb to hCD40 plus hIL-4-stimulated 2E2 B cells expressing GFP or GFP–difopein. Depicted are the quantified and normalized signals of complex A and A′ consisting of 14-3-3 and $[5′\text{-AGCT-}3′]_3$–24 bp. (**d**) ChIP assays involving crosslinked chromatin from 4B6 B cells expressing GFP or GFP–difopein and Ab to 14-3-3 or AID, and specifying Sμ, Sγ1, Sα (Sα1/Sα2) and Cμ region DNA (left panels); and ChIP assays involving chromatin from 2E2 B cells expressing GFP or GFP–difopein after stimulation by mAb to hCD40 plus hIL-4, and specifying Sμ, Sγ1, Cμ and *PAX5* DNA after precipitation by Ab to 14-3-3 or AID (right panels). DNA signals were quantified using ImageJ. Depicted is the percentage of input S region DNA precipitated by Ab to 14-3-3 or AID (mean and s.e.m. of three independent experiments).

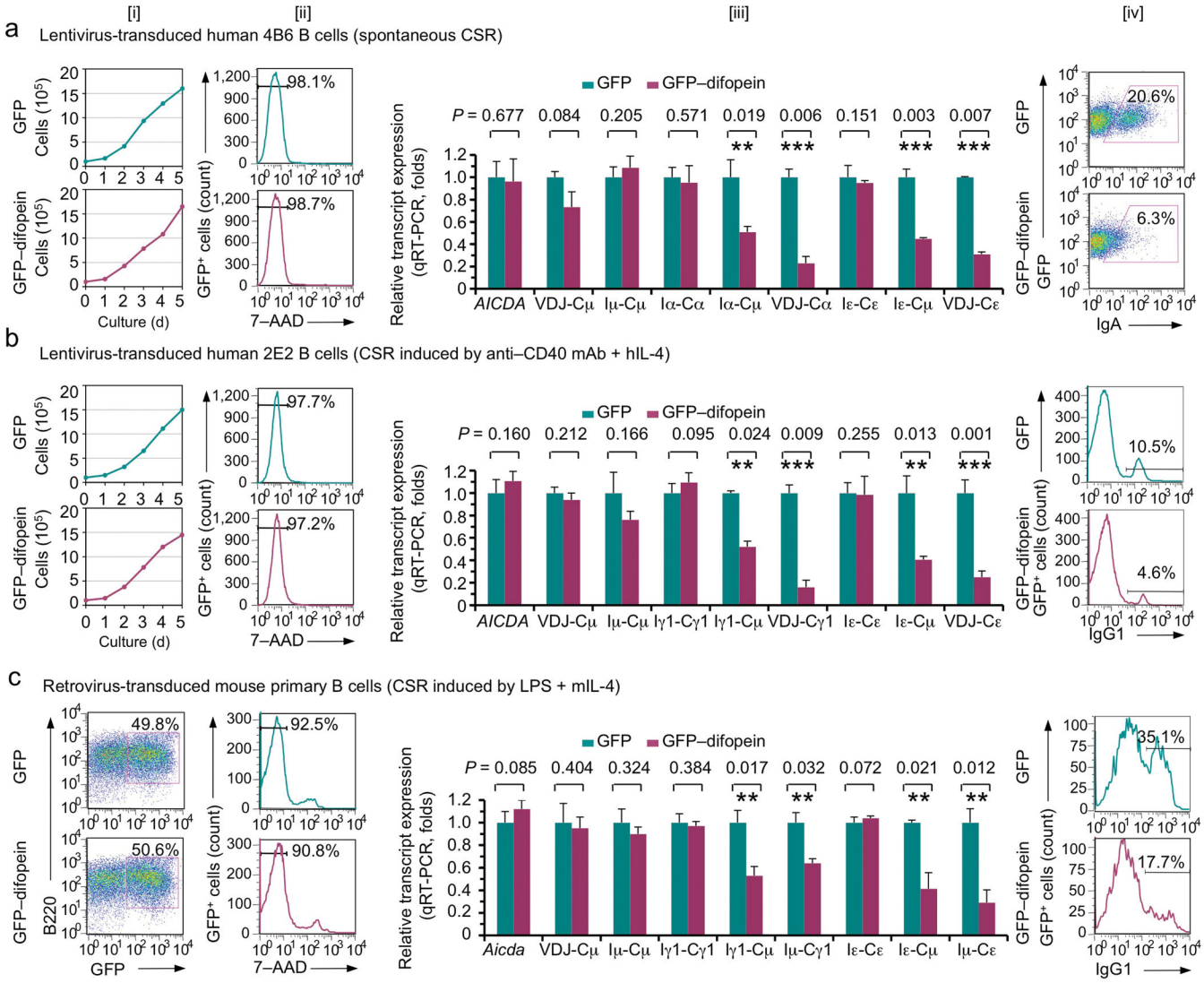

Figure 5.

Blocking 14-3-3 by difopein inhibits CSR in human and mouse B cells. (**a,b**) Human 4B6 and 2E2 B cells expressing GFP or GFP–difopein were analyzed for live B cell counts (proliferation) over a 5-d culture (panels [i]), viability (7–AAD$^-$, panels [ii]), levels of *AICDA*, mature V_HDJ_H-Cμ, germline transcripts, circle transcripts and mature post-recombination transcripts by real-time qRT-PCR (panels [iii], data are normalized to the level of *GAPDH* transcripts and depicted as ratio of the expression in GFP–difopein-expressing B cells to that in GFP–expressing B cells, mean and s.d. of triplicate samples), and surface IgA (4B6 B cells) or IgG1 (2E2 B cells) expression (panels [iv], one representative of four independent experiments). (**c**) Purified mouse primary B cells transduced with pTAC–GFP or pTAC–GFP–difopein retrovirus and then stimulated by LPS plus mIL-4 were analyzed for the proportion (GFP$^+$), number and viability of B cells expressing GFP or GFP–difopein (panels [i] and [ii]), expression of *Aicda*, mature $V_{J558}DJ_H$-Cμ transcripts, germline transcripts, circle Iγ1-Cμ and post-recombination Iμ-Cγ1 transcripts by real-time qRT-PCR and that of circle Iε-Cμ and post-recombination Iμ-Cε

transcripts by semi-quantitative RT-PCR (panels [iii], data are normalized to the level of *Gapdh* transcripts and depicted as ratio of the expression in pTAC–GFP–difopein-transduced B cells to that in pTAC–GFP–transduced B cells, mean and s.d. of triplicate samples), and surface IgG1 expression (panel [iv], one representative of three experiments). **, $p < 0.05$; ***, $p < 0.01$.

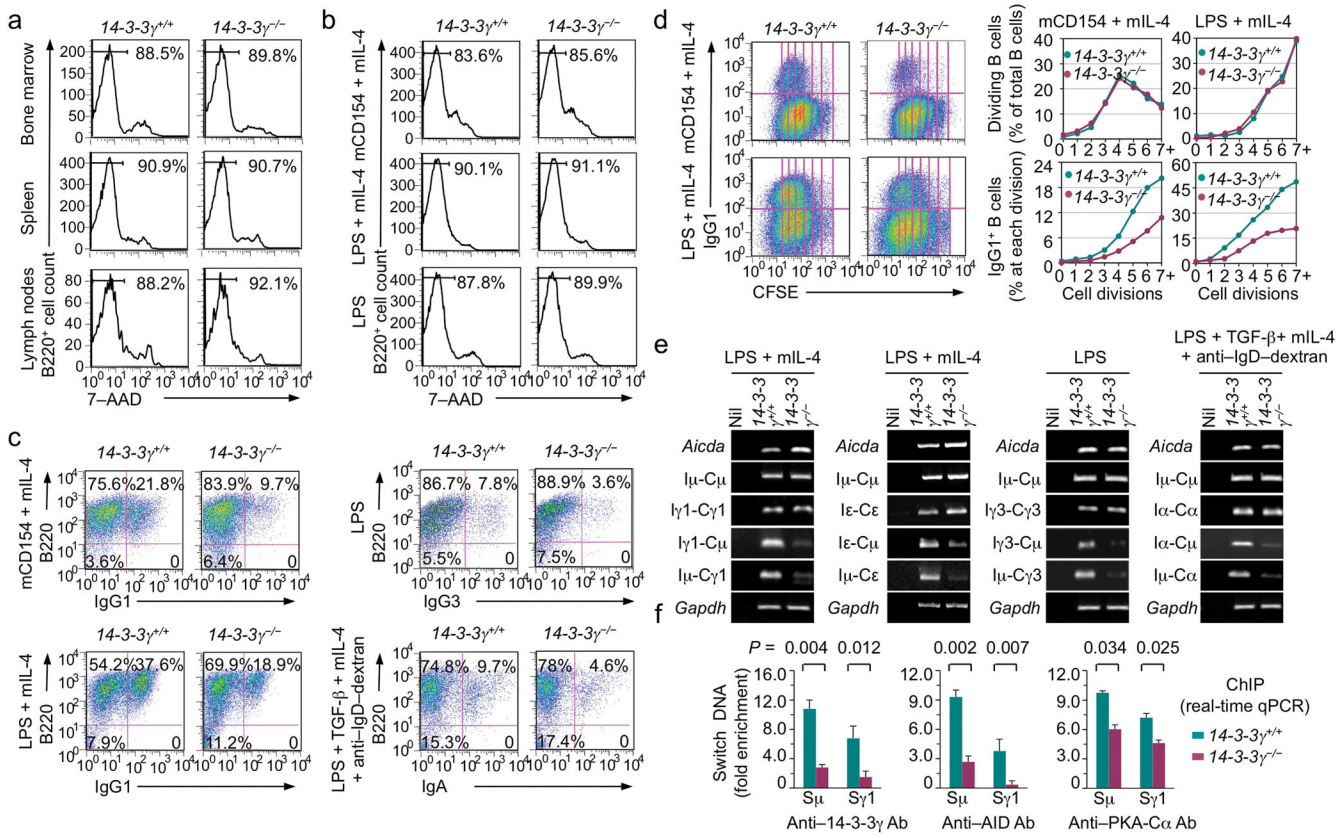

Figure 6.

14-3-3γ deficiency impaired CSR in mouse primary B cells. (**a,b**) Flow cytometry analysis of viability of *14-3-3γ*$^{+/+}$ and *14-3-3γ*$^{-/-}$ B cells (B220^{+}) from bone marrow, spleen and lymph nodes (**a**), and spleen B cells after stimulation by mCD154 or LPS plus mIL-4, or LPS alone (**b**). (**c**) Flow cytometry analysis of CSR in *14-3-3γ*$^{+/+}$ and *14-3-3γ*$^{-/-}$ B cells (one representative of three experiments). The mean and s.e.m. of CSR to each Ig isotype in *14-3-3γ*$^{+/+}$ vs *14-3-3γ*$^{-/-}$ B cells were as follows: mCD154/mIL-4-induced CSR to IgG1, 22.5±2.7% vs 10.2±0.5%; LPS/mIL-4-induced CSR to IgG1, 39.8±4.1% vs 15.2±4.3%; LPS-induced CSR to IgG3, 7.4±0.6% vs 3.4%±0.7%; and LPS, TGF-β, mIL-4 plus anti–IgD–dextran-induced CSR to IgA, 9.5±2.7% vs 4.1±0.8%. (**d**) Flow cytometry analysis of CFSE intensity and surface IgG1 expression in *14-3-3γ*$^{+/+}$ and *14-3-3γ*$^{-/-}$ B cells labeled with CFSE and stimulated by mCD154 or LPS plus mIL-4 for 4 d (left panels). Proportion of B cells completing each cell division (proliferation) and the proportion of surface IgG1^{+} B cells at each cell division are depicted (right panels). (**e**) RT-PCR analysis of germline I_H-C_H, circle I_H-Cμ and post-recombination Iμ-C_H transcripts in *14-3-3γ*$^{+/+}$ and *14-3-3γ*$^{-/-}$ B cells stimulated by LPS plus mIL-4, LPS, or LPS, TGF-β, mIL-4 plus anti–IgD–dextran. Nil: PCR reactions without DNA templates. (**f**) ChIP assays involving chromatin from *14-3-3γ*$^{+/+}$ and *14-3-3γ*$^{-/-}$ B cells after stimulation by LPS plus mIL-4 for 60 h and Ab to 14-3-3γ, AID or PKA-Cα, and quantifying Sμ and Sγ1 DNA (expressed as fold enrichment over DNA precipitated by irrelevant IgG, mean and s.d. of triplicate samples).

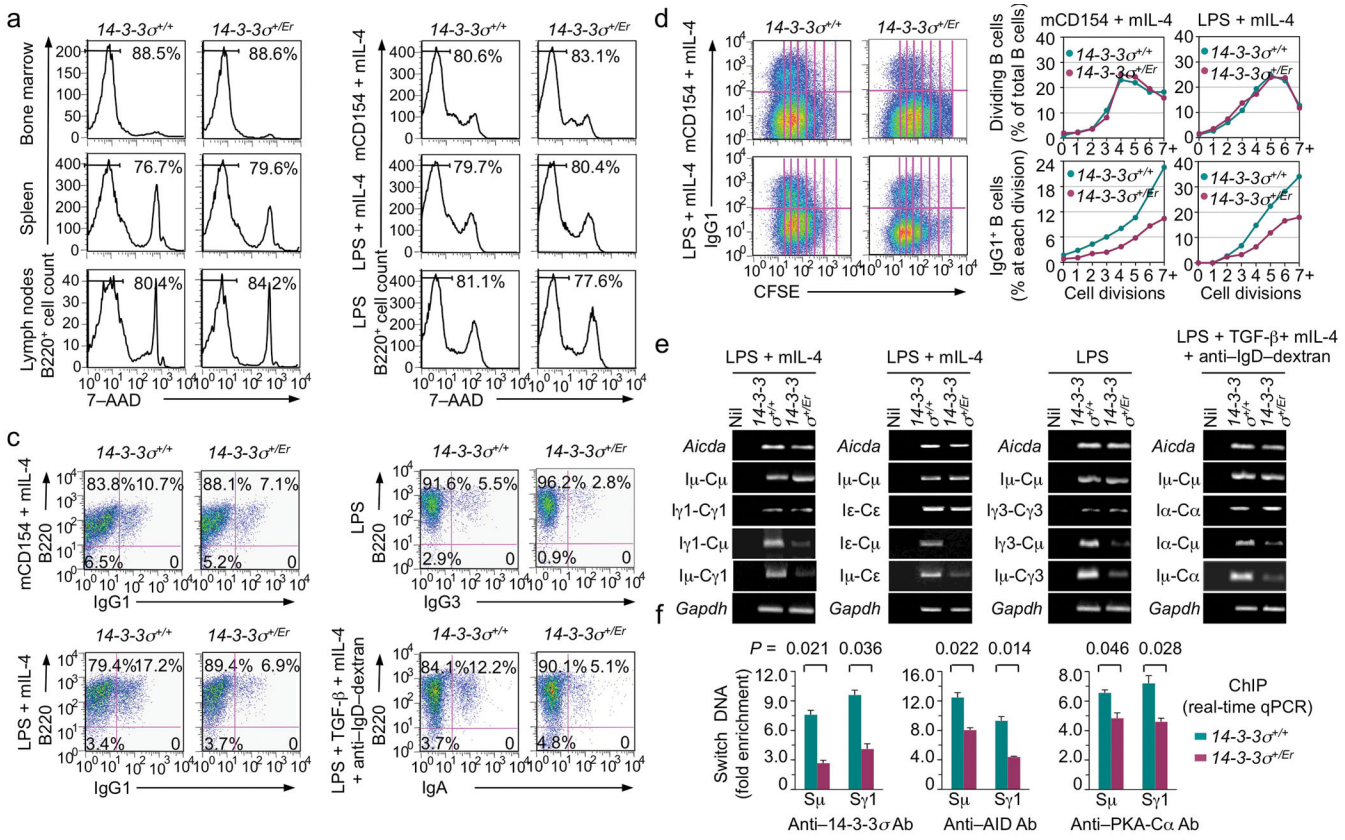

Figure 7.

14-3-3σ Er DN mutant impaired CSR in mouse primary B cells. (**a,b**) Flow cytometry analysis of viability of *14-3-3σ*$^{+/+}$ and *14-3-3σ*$^{+/Er}$ B cells (B220^{+}) from bone marrow, spleen and lymph nodes (**a**), and spleen B cells after stimulation by mCD154 or LPS plus mIL-4, or LPS alone (**b**). (**c**) Flow cytometry analysis of CSR in *14-3-3σ*$^{+/+}$ and *14-3-3σ*$^{+/Er}$ B cells (one representative of three experiments). The mean and s.e.m. of CSR to each Ig isotype in *14-3-3σ*$^{+/+}$ vs *14-3-3σ*$^{+/Er}$ B cells were as follows: mCD154/mIL-4-induced CSR to IgG1, 10.3±1.9% vs 6.0±1.8%; LPS/mIL-4-induced CSR to IgG1, 17.5±2.1% vs 7.2±1.3%; LPS-induced CSR to IgG3, 5.4±0.2% vs 2.4%±0.5%; and LPS, TGF-β, mIL-4 plus anti–IgD–dextran-induced CSR to IgA, 11.5±2.7% vs 5.8±1.9%. (**d**) Flow cytometry analysis of CFSE intensity and surface IgG1 expression in *14-3-3σ*$^{+/+}$ and *14-3-3σ*$^{+/Er}$ B cells labeled with CFSE and stimulated by mCD154 or LPS plus mIL-4 for 4 d (left panels). Proportion of B cells completing each cell division (proliferation) and the proportion of surface IgG1^{+} B cells at each cell division are depicted (right panels). (**e**) RT-PCR analysis of germline I_H-C_H, circle I_H-Cμ and post-recombination Iμ-C_H transcripts in *14-3-3σ*$^{+/+}$ and *14-3-3σ*$^{+/Er}$ B cells stimulated by LPS plus mIL-4, LPS, or LPS, TGF-β, mIL-4 plus anti–IgD–dextran. (**f**) ChIP assays involving chromatin from *14-3-3σ*$^{+/+}$ and *14-3-3σ*$^{+/Er}$ B cells after stimulation by LPS plus mIL-4 for 60 h and Ab to 14-3-3σ, AID or PKA-Cα, and quantifying Sμ and Sγ1 DNA (expressed as fold enrichment over DNA precipitated by irrelevant IgG, mean and s.d. of triplicate samples).

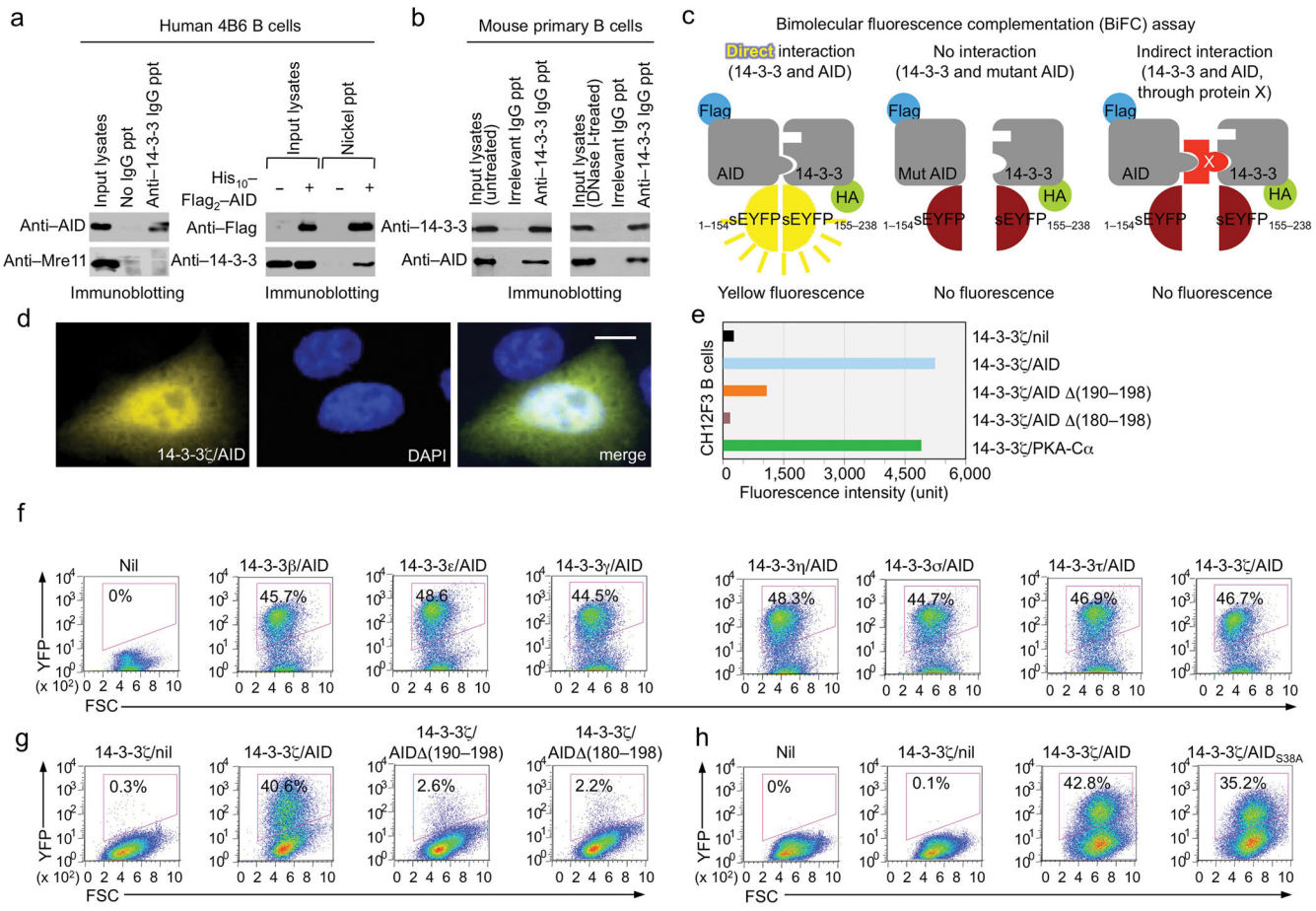

Figure 8.

14-3-3 adaptors interact directly with AID. (**a**) Immunoprecipitation of human 4B6 B cell lysates by rabbit Ab to 14-3-3 followed by immunoblotting with mouse mAb to AID or Mre11 (left); and pull-down of 14-3-3 with AID double-tagged with His_{10}–$Flag_2$ by Ni-NTA-conjugated agarose beads (right). (**b**) Immunoprecipitation of lysates of mouse primary B cells (stimulated by LPS plus mIL-4 for 48 h) by rabbit Ab to 14-3-3 followed by immunoblotting with mouse mAb to 14-3-3 or AID (left). Pre-treatment of lysates with DNase I yielded comparable results (right). (**c**) Schematics of the principle of the BiFC assay. (**d**) BiFC assays of the direct interaction of 14-3-3ζ and AID in HeLa cell nucleus, as revealed by fluorescence microscopy (also presented in Supplementary Fig. 7c). (**e**) BiFC assays of the direct interaction of 14-3-3ζ with PKA-Cα and AID, but not AIDΔ(190–198) or AIDΔ(180–198) in mouse CH12F3 B cells stimulated by LPS, mIL-4 plus TGF-β, as quantified by spectrofluorometry. (**f**) BiFC assays of the direct interaction of each of the seven 14-3-3 isoforms (fused to $sEYFP_{155–238}$) with AID (fused to $sEYFP_{1–154}$) in HeLa cells. Nil: co-expression of HA–$sEYFP_{155–238}$ and Flag–$sEYFP_{1–154}$, as analyzed by flow cytometry. (**g**) BiFC assays of the direct interaction of 14-3-3ζ with AID, but not AIDΔ(190–198) or AIDΔ(180–198) in HeLa cells (one representative of four experiments). (**h**) BiFC assays of the direct interaction of 14-3-3ζ with AID and AID_{S38A} in HeLa cells (one representative of four experiments).

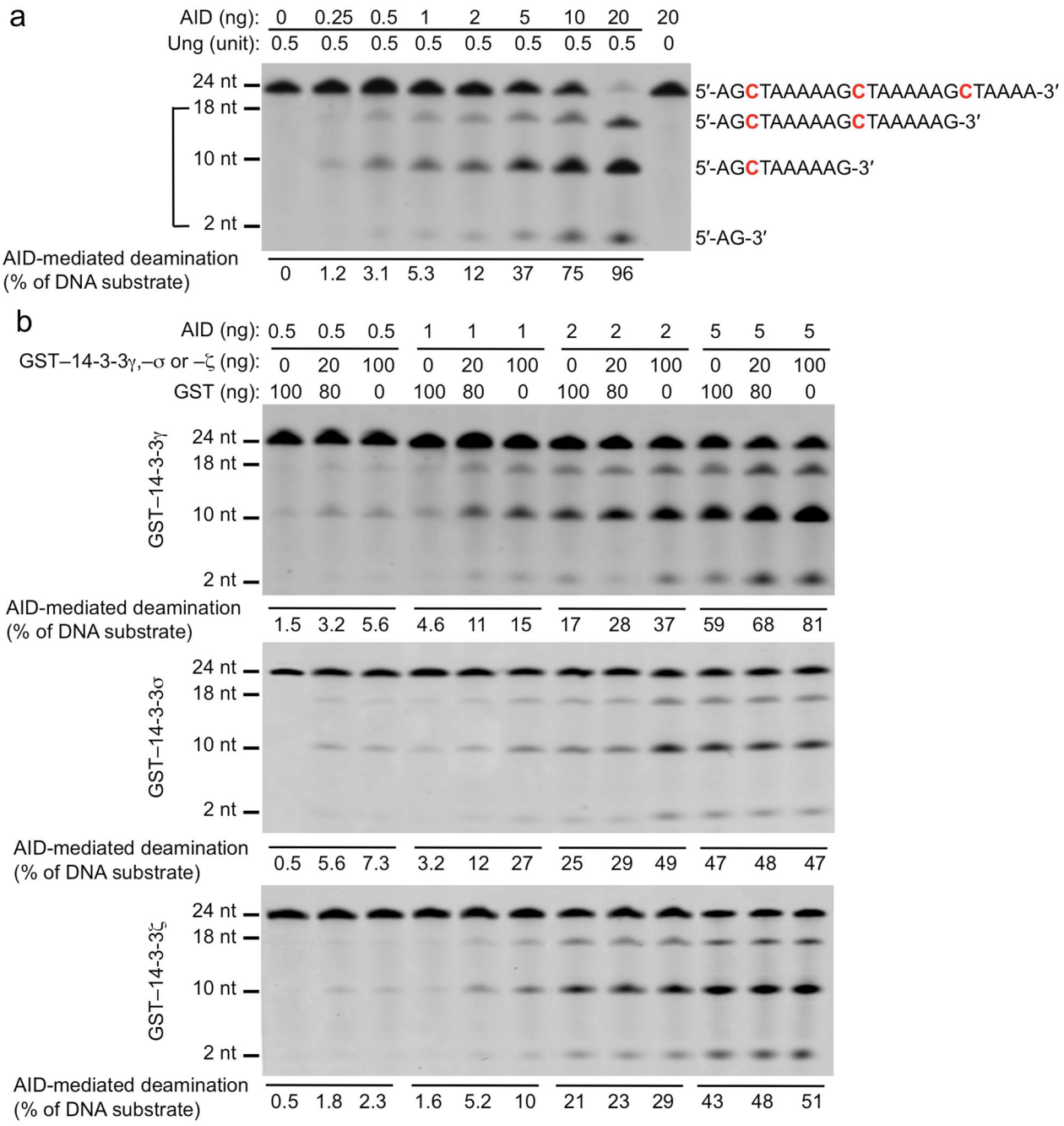

Figure 9.

14-3-3 adaptors enhance AID-mediated DNA deamination. (**a**) AID deaminated dC residues of Alexa Fluor 647-labeled [5′-AGCT-3′]$_3$–24 nt in a dose-dependent fashion. Numbers below each lane indicate the percentage of DNA substrate showing deamination (sum of three cleavage products over the total input DNA). Lack of Ung in the reaction led to no cleavage products. (**b**) DNA deamination by sub-optimal amounts of AID in the presence of purified recombinant GST–14-3-3γ (top panel), GST–14-3-3σ (middle panel) and GST–

14-3-3ζ (bottom panel). Numbers below each lane indicate the percentage of DNA substrate deaminated.